Puertes, C.; Bautista, I.; Lidón, A.; Francés, F. (2021). Best management practices scenario analysis to reduce agricultural nitrogen loads and sediment yield to the semiarid Mar Menor coastal lagoon (Spain). Agricultural Systems. 188:1-17. https://doi.org/10.1016/j.agsy.2020.103029

Best management practices scenario analysis to reduce agricultural nitrogen loads and sediment yield to the semiarid Mar Menor coastal lagoon (Spain)

Cristina Puertes[1], Inmaculada Bautista[1], Antonio Lidón[1] and Félix Francés[1]

[1]Research Institute of Water and Environmental Engineering (IIAMA), Universitat Politècnica de València, Camino de Vera s/n, E-46022 Valencia, Spain

Corresponding author: Cristina Puertes (cripueca@cam.upv.es)

Abstract

Agriculture is a major source of diffuse pollution, where nitrogen and sediment pollution of water bodies are its main associated environmental impacts. Best management practices are effective tools for preventing and minimizing water pollution. Water quality models and model-based scenario analyses are useful tools for assessing impacts of best management practices and to identify appropriate strategies on the watershed scale. This study was conducted in the southernmost Mar Menor basin, one of the largest saltwater coastal lagoons in Europe and threatened by diffuse nutrient and sediment export from the agricultural landscape. This study evaluates the impact of several management practices on nitrogen and sediment loads, and horticultural crop yield, to identify an appropriate management strategy on the watershed scale. Both structural and nonstructural management practices scenarios were evaluated: three scenarios representing field operations, two coastal line buffers, a new fertilizer management strategy and a change in the productive cultivation system from three-crop rotation to two-crop rotation. Each management practice reduced a certain type of diffuse pollution and, therefore, a combined set of changed management practices is necessary to cope with all agricultural pollution types. Contour farming, combined with hedgerow field borders, was effective in sediment yield and surface organic nitrogen export reduction terms, while improved fertilizer management reduced surface nitrate export and leaching with minimal impacts on crop yields.

Keywords

Best management practices; Nitrogen loss; Sediment yield; Semiarid; Mar Menor coastal lagoon

Highlights

- Contour farming and hedgerow borders reduce sediment and organic nitrogen export
- Effective fertilizer management practices reduce surface nitrogen export and leaching
- Combined scenarios are necessary to cope with all agricultural pollution sources

1 Introduction

Diffuse pollution is defined as the result of emissions whose source cannot be traced (La Nauze and Mezzetti, 2019), and play a key role in the degradation of aquatic environments (La Nauze and Mezzetti, 2019; Zhang et al., 2016). Agriculture has been recognized as a major source of diffuse pollution (Causapé et al., 2004; Liu et al., 2013; Rao et al., 2009) and its main associated environmental impacts are nitrogen and sediment pollution of water bodies (Zhang et al., 2014). Nitrogen inputs to aquatic environments produce their eutrophication by stimulating harmful algal blooms (Álvarez et al., 2017; Le Moal et al., 2019), while sediment inputs contribute to their habitat degradation and biota impairment (Collins et al., 2011; Mtibaa et al., 2018). Nevertheless, the use of excessive fertilizer doses (Pardo et al., 2017; Poch-Massegú et al., 2014) and poor support conservation practices (Panagos et al., 2015) are still common practices in agricultural areas.

As a result, many water policy instruments have been developed (Ingram, 2008), but water body pollution is still a problem in many parts of the world and an ongoing concern in Europe (Harrison et al., 2019). The use of fertilizers is expected to increase due to growing needs of food, fibre, feed and biofuel as a results of population growth and improved living standards (Chukalla et al., 2018; Tilman et al., 2011, 2002), whereas climate change is expected to impact hydrology and to diffuse nutrient export from agricultural areas (Wagena and Easton, 2018). Thus, developing strategies to improve the sustainability of intensive agricultural production is a major challenge (Pradhan et al., 2015; Quemada et al., 2013).

Best management practices have been recognized as effective tools for preventing or minimizing pollution from agricultural areas (Chiang et al., 2014; Giri and Nejadhashemi, 2014). These include soil and water conservation practices and management techniques (Sharpley et al., 2006) whose objective is to control and reduce sediment and nutrient sources. Nonetheless, their effectiveness varies between sites and soil type, and testing them through field studies is unfeasible because they are costly and time consuming (Qiu et al., 2018; Sith et al., 2019; Strauch et al., 2013). Therefore, water quality models and model-based scenario analyses are useful tools for assessing their impact and identifying the appropriate strategy to devise watershed management plans (Cavero et al., 2012; Dechmi and Skhiri, 2013; Ullrich and Volk, 2009).

In this study, the effectiveness of several management practices was assessed with the distributed conceptual hydrological model TETIS (Francés et al., 2007), for which a nitrogen sub-model was developed, TETIS-N. The study lay in the southernmost Mar Menor basins, dominated by agricultural lands and characterized by a semiarid climate. The Mar Menor is one of the largest saltwater coastal lagoons of Europe, which provides

aesthetic, touristic, fishing and recreational opportunities with a high environmental value. This value has been internationally recognized because it is on the List of Wetlands of International Importance (RAMSAR) and on the List of Specially Protected Areas of Mediterranean Importance (SPAMIs). It has also been declared a Site of Community Importance (SCI) and a Special Protection Area for Birds (SPA). However, these protection regulations have failed to prevent its deterioration (Garcia-Ayllon, 2018). Urbanization, tourism and intensive agricultural activity have been recognized as the main causes of pollution (García-Ayllón and Miralles, 2014; Rey et al., 2013), but being one of the main horticultural productive areas in Europe (Álvarez-Rogel et al., 2006), diffuse nutrient export from the agricultural landscape is the main environmental impact (Perni and Martínez-Paz, 2013).

Accordingly, several studies have been conducted (e.g., De Pascalis et al., 2012; León et al., 2017; Tsakovski et al., 2009; Velasco et al., 2006), but very little attention has been paid to evaluate mitigation measures (e.g., Alcolea et al., 2019; Perni and Martínez-Paz, 2013). Jiménez-Martínez et al. (2016) recognized groundwater discharge (direct discharge from aquifers to the lagoon) as the main source of nutrients, and established the implementation of improved agricultural practices to reduce nitrate leaching as a critical measure. Alcolea et al. (2019) assessed two mitigation measures in order to reduce this groundwater nutrient discharge, new drains to intercept groundwater discharge and distributed groundwater pumping. Unfortunately, Alcolea et al. (2019) showed that both measures were able to reduce groundwater discharge, and consequently, nitrate discharge, but neither was able to maintain nitrate discharge below tolerable levels (nitrate concentrations above the 50 mg NO_3^- L^{-1} limit, as set out in the Nitrate Directive of the European Commission (91/676/EEC)). Hence, additional and complementary measures, especially those that focus on reducing nitrogen leaching, are necessary.

In this context, a baseline scenario, which represents the current situation, and seven scenarios consisting in the application of different management practices have been evaluated. They are: three scenarios to change field operation management strategies (contour farming and contour farming combined with grassy field borders and hedgerow field borders), two coastal line buffers (100 m and 500 m), a new fertilizer management strategy based on simple soil-plant nitrogen mass balance, and this fertilizer management strategy combined with a change in the productive cultivation system from three-crop rotation to two-crop rotation. The objective of this study is twofold. First, it aims to evaluate the impact of these management practices on nitrogen and sediment loads, and their impact on horticultural crop yield. Second, it also intends to serve as a springboard to identify an appropriate management strategy on the watershed scale,

which will be applied to another watershed with similar characteristics and similar problems, as very few studies have been conducted in semiarid and coastal environments (Hashemi et al., 2016).

2 Materials and Methods

2.1 Study area

The study area lay in the southernmost Mar Menor basins in southeast Spain (Figure 1), where only agricultural influence exists. This area covers 100.1 km^2 and is divided into 88 basins (66 of which are small coastal basins) and six endorheic basins. All the basins are ephemeral rivers, and no gauging stations are located in the area.

Figure 1 Location of the study area.

Altitude ranges from 0 to 393 m a.s.l. (Figure S1) and climate is semiarid, with a mean annual precipitation of 291 mm, a mean annual reference evapotranspiration of 1061 mm (Hargreaves and Samani, 1985) and a mean annual temperature of 18.7 °C (for the 1971-2016 period). Soils are mainly Xerosols, Arenosols and Lithosols, and loam and clay loam are the most frequent textural classes. The underlying materials are mainly Quaternary-aged with a thickness from 50 to 150 m and outcrops of Pliocene- and Miocene-aged materials.

Most of the study area is used for agricultural land use (53.3%), with citrus trees and horticultural crops being the dominant land uses (Figure 2 and Table 1). The commonest

agricultural practice consists of annual three-crop rotation among broccoli, melon and lettuce. This area is also characterized by the use of high fertilizer doses (a common problem in Spain's irrigated Mediterranean areas (Calatrava et al., 2011; De Paz and Ramos, 2002). Daily fertigation by a drip irrigation system and no contouring is carried out.

Figure 2 Simplified land use map of the study area.

Land use	Area (%)
Continuous urban fabric	3.33
Discontinuous urban fabric	5.20
Mineral extraction sites	6.01
Dump sites	0.83
Construction sites	0.77
Sport and leisure facilities	2.44
Non-irrigated arable land	4.50
Permanently irrigated arable land	36.67
Fruit trees and berry plantations	9.48
Complex cultivation patterns	1.50
Principally agricultural land	1.17
Coniferous forest	2.35
Sclerophylous vegetation	16.04
Transitional woodland	3.16
Beaches, dunes and sand plains	2.17
Sparsely vegetated areas	2.21
Salt marshes	1.56
Salt evaporation ponds	0.61

Table 1 Area (%) for each land use in the study area.

Hence, in order to cope with the problems of diverse land use distributions, a distributed model, which divides the area into cells, downscales the environmental variables to each cell, simulates the state variable in each cell and assembles the results for the complete basin. It stands out as an appropriate tool.

2.2 TETIS model description

TETIS-N is a hydrological distributed conceptual model composed of three sub-models: hydrology (Francés et al., 2007), sediment transport (Bussi et al., 2014, 2013) and nitrogen transport and transformation (developed and described in this study). The three sub-models are described as follows.

2.2.1 Hydrological sub-model

In TETIS-N, each cell is hydrologically represented by five vertical connected tanks (Figure 3) and a channel tank. T_0 represents the interception process (only evaporation) and T_1 refers to soil static storage (i.e., below field capacity), where evapotranspiration is the only output from this tank. Then water moves downwardly as long as the tank vertical outflow capacity is not exceeded. T_2 is superficial water storage and T_3 is gravitational storage (i.e., above field capacity). Both represent the surface runoff process (overland flow and interflow, respectively). The last tank, T_4, represents the aquifer. These three tanks (T_2, T_3 and T_4) act as simple linear reservoirs and their outflows are routed to the corresponding tank of the downstream cell. T_5 represents the river netflow.

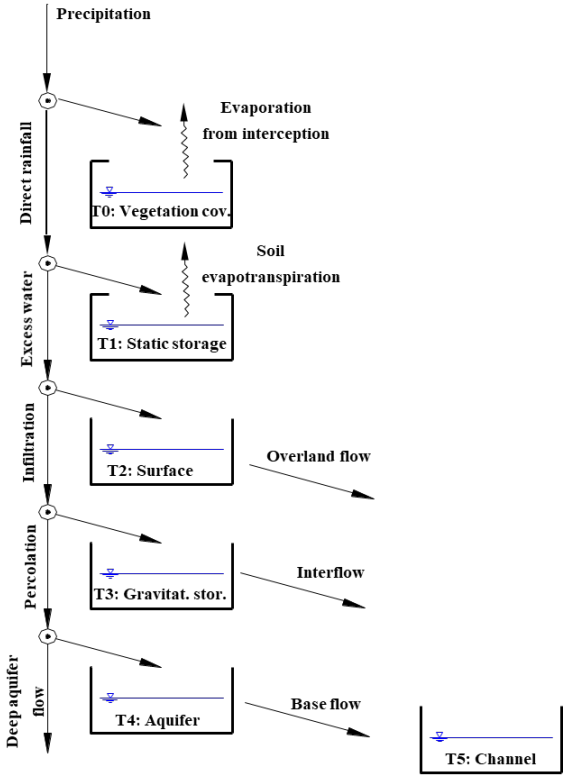

Figure 3 Vertical conceptualization of TETIS.

Two thresholds characterize the horizontal conceptualization of TETIS-N, which divides cells into hillslope, gully and river channel cells (Figure 4). Overland flow and interflow, are routed to the T_2 and T_3 tanks of the downstream cell, unless they reach a gully cell, in which case, flows are routed to the river channel tank, T_5. Likewise, the base flow is routed to the downstream T_4 cell, until it reaches a river channel cell, in which

case, it is also routed to T_5. The flow routing along the stream river network is computed by the Geomorphologic Kinematic Wave methodology (Francés et al., 2007).

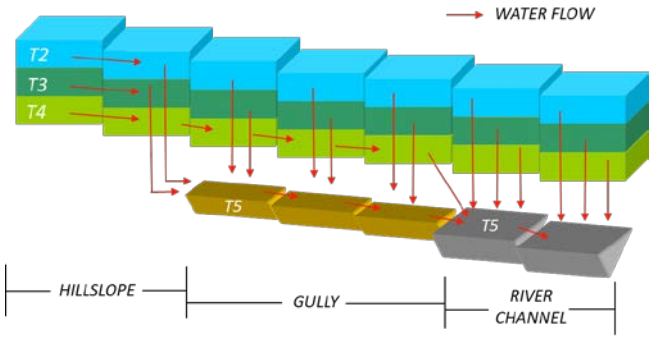

Figure 4 Horizontal conceptualization of TETIS.

Three types of irrigation methods are considered in TETIS: drip, sprinkler and flood irrigation. Drip and flood irrigation are directly added to the direct rainfall flux (Figure 3), while sprinkler irrigation is added to the precipitation flux (Figure 3).

Evapotranspiration in TETIS is calculated as:

$$Evapotranspiration = Min[ET_0 * \lambda_v(m) * R_2 \,;\, T_1] \qquad Eq(1)$$

where ET_0 is the potential evapotranspiration, $\lambda_v(m)$ is the vegetation cover index or crop coefficient (with annual periodicity and a different value for each month m), R_2 is a correction factor and T_1 is the water in static storage.

2.2.2 Sediment sub-model

In the sediment sub-model, each cell is represented by three vertical tanks (Figure 5). Sediment particles are divided into sand, silt and clay, and each one with a representative grain diameter and settling velocity. Sediment availability and sediment transport capacity control these processes: sediment production, transport and deposition.

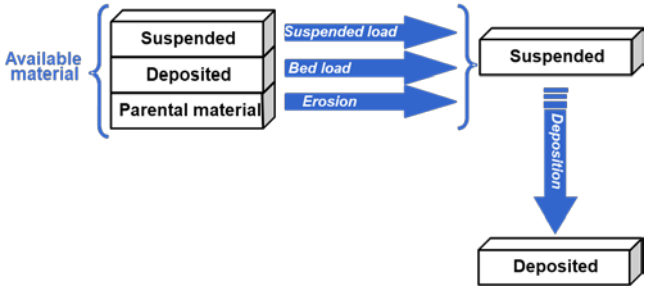

Figure 5 Sediment conceptualization of TETIS.

Hillslope sediment transport capacity is calculated by the modified Kilinc and Richardson equation (Julien, 2010; Kilinc and Richardson, 1973). It incorporates the effect of soil characteristics, land use and agricultural management practices by means of the soil erodibility factor (K factor), the cover-management factor (C factor) and the support practice factor (P factor) of the Universal Soil Loss Equation (USLE) (Wischmeier

and Smith, 1978). This transport capacity is first used to transport suspended sediments downstream. Then the residual transport capacity is employed to mobilize deposited sediments and to finally erode parent soil (Figure 5). River channel transport is computed by means of the Engelund and Hansen equation (Engelund and Hansen, 1972) and it is first used to route suspended sediments downstream and the residual transport capacity is employed to mobilize deposited sediments.

2.2.3 Nitrogen sub-model

The general conceptualization of the TETIS-N nitrogen sub-model is based on the formulation of the model INCA-N (Wade et al., 2002) and it includes a crop growth module based on EU-Rotate_N (Rahn et al., 2010). In TETIS-N the nitrogen cycle is simulated as in INCA-N, although some new features were developed in this study. First, TETIS-N incorporates the modelling of organic nitrogen. Second, it considers NH_4^+ soil sorption. Finally, this sub-model was coupled to the sediment sub-model. This last improvement allowed the transport of the nitrogen fixed to sediments to be simulated. In order to improve the simulation of the nitrogen plant uptake in agricultural areas, the model uses the formulation employed in EU-Rotate_N to simulate crop growth and, consequently, crop yield.

Each cell is represented by ten tanks (Figure 6). Four tanks and seven processes represent the nitrogen cycle in soil. Mineralization, immobilization, nitrification and denitrification are represented by first-order kinetics. By way of example, the mineralization process is described as:

$$Min = k_{Min} f(t) f_{Min}(\vartheta) OrgN \qquad Eq(2)$$

where *Min* is the NH_4^+ mineralized mass (kgN day^{-1}), k_{Min} is the mineralization rate constant (day^{-1}), $f(t)$ is a dimensionless term that accounts for the soil temperature influence, $f_{Min}(\vartheta)$ is a dimensionless term that accounts for the soil water content influence (for the mineralization process in this example) and *OrgN* is organic nitrogen content (kgN). As volatilization is mainly a pH-dependent process, for simplicity reasons, it is described by a first-order kinetic with neither temperature nor water content correction. NH_4^+ adsorption and desorption by clay colloids are also modelled in the simplest way, by a linear sorption isotherm:

$$c_s = k_d c_L \qquad Eq(3)$$

where c_s is the N-NH_4^+ concentration in the sorbed phase (mgN kg^{-1}), k_d is the NH_4^+ distribution coefficient (dm^3 kg^{-1}) and c_L is the N-NH_4^+ concentration in solution (mgN dm^{-3}).

Four tanks and two processes (nitrification and denitrification) represent the in-stream nitrogen cycle. These processes are also represented by first-order kinetics, but only

account for temperature influence, $f(t)$. The nitrogen cycle in the aquifer is represented by two tanks and no process is simulated because not biological activity is considered.

Soil water correction functions are based on those proposed in Brady and Weil (2002). Mineralization and immobilization are corrected according to:

$$f(\vartheta)_{Min} = \begin{cases} 0 & \vartheta \le \vartheta_{wp} \\ (\vartheta - \vartheta_{wp})/(\vartheta_{fc} - \vartheta_{wp}) & \vartheta_{wp} \le \vartheta \le \vartheta_{fc} \\ \vartheta_{fc}/\vartheta & \vartheta > \vartheta_{fc} \end{cases} \quad Eq(4)$$

where ϑ is soil moisture (cm cm^{-1}), ϑ_{wp} is soil moisture at the wilting point (cm cm^{-1}) and ϑ_{fc} is soil moisture at field capacity (cm cm^{-1}). The nitrification process is corrected according to:

$$f(\vartheta)_{Nit} = \begin{cases} \vartheta/\vartheta_{fc} & \vartheta \le \vartheta_{fc} \\ (1-\vartheta)/(1-\vartheta_{fc}) & \vartheta > \vartheta_{fc} \end{cases} \quad Eq(5)$$

And, finally, the denitrification process is corrected according to:

$$f(\vartheta)_{De} = \begin{cases} 0 & \vartheta \le \vartheta_{fc} \\ (\vartheta - \vartheta_{fc})^2/(1-\vartheta_{fc})^2 & \vartheta > \vartheta_{fc} \end{cases} \quad Eq(6)$$

The temperature correction function (Wade et al., 2002) for both soil and in-stream parameters is:

$$f(t) = \beta^{(T-T_{opt})} \quad Eq(7)$$

where β is a constant with a typical value of 1.047, T is air or soil temperature (°C) and T_{opt} is the optimum temperature (°C), which usually takes a value of 20°C.

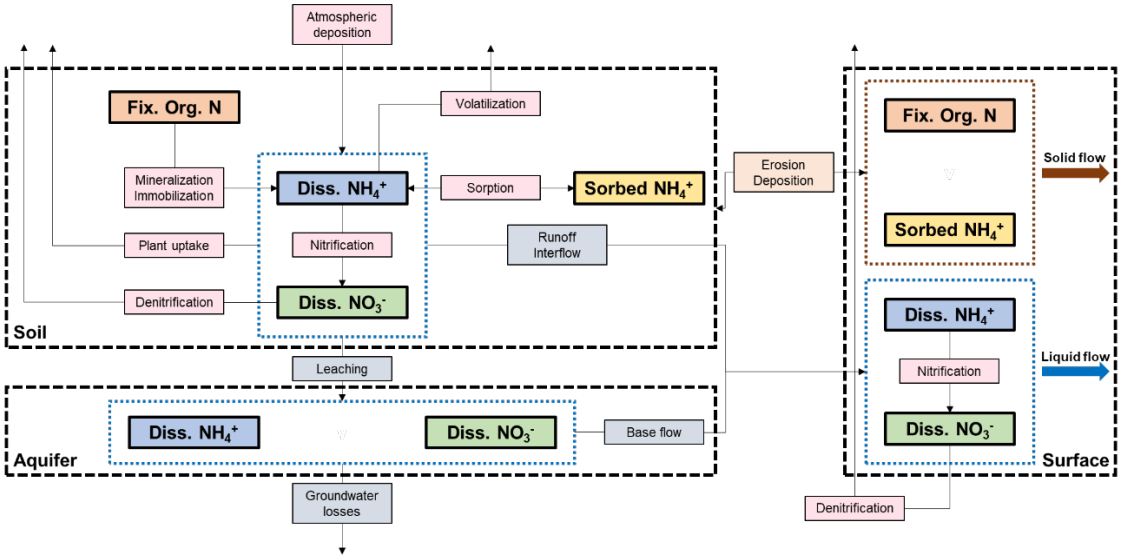

Figure 6 Nitrogen conceptualization of TETIS.

Nitrogen plant uptake is divided into two steps (Porporato et al., 2003). Passive uptake is calculated as an advective movement proportional to the transpiration flux, which is calculated through the vegetation cover factor. If this uptake does not fulfil the requirement (i.e., daily potential uptake), a diffusive component is considered (i.e., active

uptake). This active uptake is proportional to nitrogen content and a diffusion coefficient. The daily potential nitrogen uptake is assumed constant all year long and is calculated from the annual nitrogen demand. In agricultural areas with nonwoody crops, the model has a specific crop growth sub-model that calculates a daily potential uptake depending on crop development.

This crop growth sub-model (Rahn et al., 2010) simulates dry matter. Every day, the increment in dry matter is corrected to account for the influence of air temperature and water and nitrogen availability. The daily nitrogen plant uptake is calculated according to the minimum nitrogen content in the crop for maximum growth (i.e., the critical nitrogen value).

Dissolved nitrogen transport to the downstream cell is carried out according to the horizontal hydrological connection between tanks and by considering only advective movement. The nitrogen fixed to sediments is considered to be fixed only to the clay fraction and is mobilized according to the clay sediment fraction that is eroded, deposited or mobilized to the downstream cell.

2.2.4 Model parameters and split parameter structure

The hydrological and sediment sub-models of TETIS-N present a split-parameter structure (Francés et al., 2007). The parameter maps and the potential evapotranspiration data series act as modal values, where the absolute value of each cell is not important. Importance lies in correct spatial distribution (or temporal with the potential evapotranspiration). These modal values are later corrected by means of a correction factor and instead of calibrating the number of parameters multiplied by the number of cells, only the correction factors should be calibrated.

The hydrological sub-model has nine correction factors: maximum static storage, evapotranspiration, infiltration, hillslope surface velocity, percolation, interflow hydraulic conductivity, deep percolation, base flow hydraulic conductivity and flow velocity.

The sediment sub-model is represented by three correction factors, one for each transport capacity (hillslope, gullies and channel). With every time step, in each cell transport capacity is calculated and is corrected by multiplying it by the corresponding correction factor.

In the nitrogen sub-model, parameters depend on the land use type. The split-parameter structure is used only for the NH_4^+ distribution coefficient, which depends on the clay content and type, and presents a correction factor. Therefore, the nitrogen sub-model presents one correction factor (the NH_4^+ distribution coefficient) and three temperature correction parameters. It also presents eight land use specific parameters (mineralization, immobilization, volatilization, nitrification and denitrification rates), a diffusion coefficient, the annual nitrogen potential uptake and the nitrogen form

preference. For channel cells, it presents two in-stream parameters: nitrification and denitrification rates. The crop growth sub-model requires information about plant and harvest date, the initial and final crop dry matters, the initial and final crop cover factor, base temperature, nitrogen form preference, and the a and b crop-specific coefficients (Rahn et al., 2010).

2.3 Model setup

2.3.1 Initial parameter estimation

The hydrological sub-model requires information on topography, land use, soil and geology. The digital elevation model (DEM) was obtained from the Spanish *Centro Nacional de Información Geográfica* (CNIG) with 5 m grid spacing. Although computation time significantly increased (4.003.244 cells had to be simulated), fine discretization was required to adequately reproduce the river network.

Slope, flow direction and flow accumulation maps were derived from the DEM, while hillslope surface velocity was calculated from the slope map according to Francés et al. (2007). CORINE Land Cover 2006 was employed as a land use map and the seasonal variation of actual evapotranspiration for each land use was introduced into the model by means of the crop coefficient. It was calculated daily for crop land uses, and monthly for other land uses according to Allen et al. (1998).

Maximum static storage (Figure S2) was calculated according to the depth available to roots (Hiederer, 2013), roots' depth and soil available water content; that is, the difference between field capacity and the wilting point. These were derived from the soil texture data (Ballabio et al., 2016) and by applying the Clapp and Hornberger (1978) equation.

Infiltration capacity at saturation (Figure S3) was calculated using the soil texture data, organic matter content (Hiederer, 2013), and Saxton and Rawls (2006) pedotransfer functions. Percolation capacity (Figure S4) was estimated from the qualitative permeability map of the *Instituto Geológico y Minero de España* (IGME). As sufficient information was lacking, the hydraulic conductivity of the interflow was taken to be the same as the saturated infiltration capacity (Francés et al., 2007).

The sediment sub-model requires information about soil textural composition (Ballabio et al., 2016) and three USLE factors (K, C and P factors). The K factor (Figure S5) was calculated according to Panagos et al. (2014) from the soil texture data. The C factor (Figure S6) was estimated according to the vegetation type using the values proposed by Alatorre et al. (2010). The P factor was set at 1 because support practices are not currently applied.

In the nitrogen sub-model, the soil organic nitrogen map (Figure S7) was calculated from the soil organic carbon content map (Hiederer, 2013). This map was transformed into soil organic nitrogen content by assuming typical soil C:N ratios: 10 for agricultural land uses and 20 for the other land uses (Weil and Brady, 2017).

The active soil depth was calculated as the minimum between the depth available to roots (Hiederer, 2013) and roots' depth, the bulk density map was obtained from Ballabio et al. (2016) and the previously calculated wilting point soil water content map was used. The NH_4^+ distribution coefficient map was calculated according to the topsoil clay content map, while seasonal variation in the vegetation cover factor for each land use was estimated according to the land use and aerial images.

Plant and harvest dates were consulted with the Water Users Association, while initial and final crop dry matter was estimated according to Gallardo et al. (2011), Rincon et al. (1999) and Suárez-Rey et al. (2016) for melon, broccoli and lettuce, respectively. The initial and final crop cover factors were estimated by taking personal experience into account. The nitrogen preference form was estimated according to Albornoz and Lieth (2016) and Britto and Kronzucker (2013). Base temperature and crop-specific coefficients a and b were obtained from Rahn et al. (2010) and adjusted to the study area characteristics.

2.3.2 Model inputs

Precipitation and temperature were obtained from the v4 version of the SPAIN02 dataset (Herrera et al., 2016), which provides daily precipitation and temperature values from 1971 to 2008. These series were extended to 2016 with the precipitation and temperature data provided by the *Agencia Estatal de Meteorología* (AEMET) of a near meteorological station in Cartagena. Due to the long simulated period and lack of better data, evapotranspiration was calculated from the temperature values according to Hargreaves and Samani (1985). Irrigation areas and volumes were obtained from the *Hydrological Watershed Plan of the Segura Region*.

Only the land uses golf course (included in the urban fabric), citrus trees and horticultural crops were considered fertilized. Rainfed crop areas were excluded because, by being a semiarid area, sowing depends on the previous precipitation amount and the area covered by these crops is small, compared to the irrigated area (Table1). The golf course fertilizer doses were obtained by consulting experts in the field (Table 2 and Figure 7). Citrus doses were obtained from the monthly advisory fertilization program of the *Sistema de Información Agraria de Murcia* (SIAM), which establishes a monthly fertilizer amount (Figure 7), and values are often respected by farmers. As the fertilizer doses are more variable for horticultural crops, values should be supplied daily to the model. The total fertilizer amounts were obtained from Ramos and Pomares (2010).

These recommended values are not currently respected and were increased to take into account excess and NO_3^- irrigation content. These final values were consulted with experts in the field and the Water Users Association (Table 2). Total values were transformed into daily values according to the growing curve of each crop (Figure 7).

Land use		Nitrogen fertilizer	Plant date	Harvest date
Golf course		226	-	-
Citrus trees		250	-	-
Horticultural crops	Broccoli	250	Jan 1	Apr 30
	Melon	130	Jun 1	Aug 31
	Lettuce	130	Oct 1	Dec 31

Table 2 Current annual fertilizer doses. Values in kgN ha^{-1} $year^{-1}$.

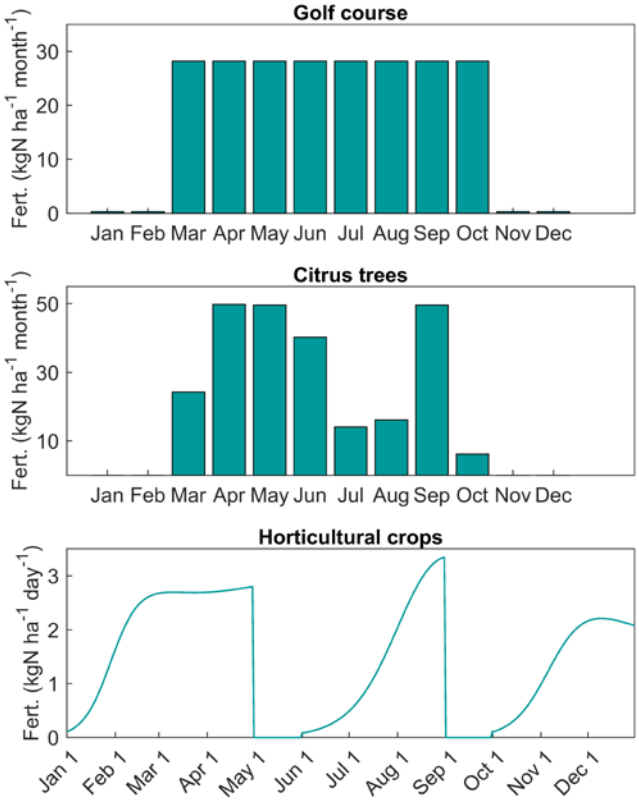

Figure 7 Fertilizer doses. Golf course, citrus trees and horticultural crops land uses

Atmospheric deposition values were obtained from García-Gómez et al. (2014). The total nitrogen atmospheric deposition in the study area was 7.5-10 kgN ha^{-1} $year^{-1}$, with an approximate nitrate:ammonium ratio of 2:1. The considered values for the study area were 3 kgN-NH_4^+ ha^{-1} $year^{-1}$ and 6 kgN-NO_3^- ha^{-1} $year^{-1}$, which were homogenously transformed into daily values.

2.4 Model implementation

The model was calibrated to represent current study area characteristics. Although they have evidently changed over the 46 years of data availability (1971-2016), these long input data series were used to obtain the model parameters, as well as

representative water, sediment and nitrogen balances of the study area's current situation. A daily time step was used and, as observed data were lacking, calibration was carried out in a non-traditional manner. Nevertheless, even if the prediction power of the model was not high, it could be used to evaluate the effectiveness of different management practices (Özcan et al., 2017a) because this process was based on comparisons and model simulations were used herein as projections of ecosystem behaviour rather than predictions.

In the hydrological sub-model, as all streams were ephemeral rivers, interest remains in surface runoff (overland flow and interflow) and percolation fluxes. Thus, as groundwater information was lacking, only the hydrological correction factors governing these were calibrated. This calibration was based on previous flood studies (CAAMA, 2016a, 2016b) carried out by the Murcia Council (*Consejería de Agua, Agricultura y Medio Ambiente de la Región de Murcia*).

Figure 8 Basin used to calibrate the hydrological and sediment sub-models.

From these flood studies, it was possible to calculate the 25-year return period outflow hydrograph of the larger basin in common (Figure 8), the volume of which was the data used to calibrate the sub-model. The model was run for the 1971-2016 period using the first year (1971) as a warm-up period. With these results, a flood frequency analysis was performed to obtain the volume of the 25-year return period hydrograph. This value was compared to the calculated one. The 25-year return period was chosen because, given the length of the data series (46 years, 1971-2016), it was not possible to use a longer return period.

In agricultural areas, evapotranspiration is a very important state variable and hence, the model's general hydrological behaviour was validated using the v3.3b satellite-based evapotranspiration data of the Global Land Evaporation Amsterdam Model (GLEAM)

(Martens et al., 2017; Miralles et al., 2011). For the horticultural crops area, the simulated evapotranspiration values (ET_{sim}) were compared to the crop evapotranspiration values under standard conditions (ET_c). These ET_c values were calculated using the ET_0 from the *Sistema de Información Agraria de Murcia* at the closest station (Cartagena, CA12) and these values were affected by the corresponding crop coefficient value (Allen et al., 1998). The ET_0 values from the *Sistema de Información Agraria de Murcia* were calculated using the observed data and applying the Penman-Monteith equation. The available data covered the 2006-2016 period.

As no sediment measurements existed, the sediment sub-model calibration was performed using the same basin (Figure 8) and based on the calculation of its mean annual erosion rate according to Wischmeier and Smith (1978). Factors K, C and P were calculated from the input model maps. Factor R (rainfall and runoff factor) was obtained from the R isoline map of the Spanish *Instituto para la Conservación de la Naturaleza* (ICONA) and the LS factor (slope-length and slope steepness factor) was obtained from Mintegui et al. (1993). Correction factors were calibrated to minimize the volume error between the simulated and calculated mean annual erosion rates. With sediment, the sub-model was markedly influenced by the initial condition (Bussi et al., 2014) and, consequently, in order to obtain a representative initial condition, the model was first run for the period 1971-2016, which was a long enough period. The obtained final condition was then used as the initial condition for the calibration period (1971-2016). The mean annual erosion rate was obtained from these results.

AS the nitrogen sub-model presented specific parameters for each land use, all the study area was used during the calibration process. The in-stream nitrogen parameters were fixed to zero because the residence time was shorter than one day (CAAMA, 2016a, 2016b) and, as no nitrogen measurements or nitrogen-related information existed for this area, the land use parameters were adjusted to accomplish the nitrogen plant potential uptake of each land use. The initial land use specific parameters values were obtained from the literature (D'Odorico et al., 2003; Jung et al., 2010; Kimmins, 2004; Rankinen et al., 2006; Wade et al., 2002; Weil and Brady, 2017). The calibration process consisted in adjusting these values to obtain a similar mean annual uptake for the 2002-2011 period to the annual plant potential uptake. The model was validated during the 2012-2016 period. Specifically, the horticultural crops parameters, which represent the largest and more interesting area, were validated by comparing the estimated crop yield target (Gallardo et al., 2011; Rincon et al., 1999; Suárez-Rey et al., 2016) and the simulated crop yield during the 2002-2016 period. The 1971-2001 period was used as a warm-up period to obtain the initial condition.

In order to obtain a representative current annual balance, the model had to be run for a long enough period. Therefore, the calibrated model was run for the 2002-2016 period and, in order to extend these results, climate repetition was assumed. Hence the model was re-run using the model inputs of the 1971-2016 period. Thus the model was finally run for a total of 61 years with the current conditions, which allowed the mean annual balances that characterize the baseline scenario to be obtained.

2.5 Best management practices scenarios and model representation

Several management practices were evaluated and in order to analyse the results, the changes in the amount of pollutants (i.e., nitrogen and sediment) were compared to the baseline scenario. The effectiveness of each scenario was computed as the percent change:

$$Percent\ change = \frac{BMP - baseline}{baseline} 100 \qquad Eq(8)$$

where *Percent change* is the percent change (%), *BMP* is the average annual pollutants load of each management practice scenario and *baseline* is the average annual pollutants load of the baseline scenario.

The management practices established in the 2017 and 2018 official regulations (CARM, 2018, 2017) were chosen to be evaluated. Less and more restrictive variations were also included as additional scenarios (additional). According to Pearce and Yates (2017) and Wang et al. (2018), management practices can be divided into structural (intercept pollutants) and nonstructural (reduce pollution). In this study, both structural and nonstructural management practices were evaluated. Eight scenarios (including the baseline scenario) were evaluated: (1) baseline; (2) contour farming (additional); (3) contour farming and grassy field borders (additional); (4) contour farming and hedgerow field borders (CARM, 2018, 2017); (5) 100 m coastal line buffer (CARM, 2018, 2017); (6) 500 m coastal line buffer (additional); (7) fertilizer management with the traditional three-crop rotation (CARM, 2017); (8) fertilizer management with two-crop rotation (CARM, 2018).

These scenarios were simulated under the same initial conditions as in the baseline scenario and for the same period: 2002-2016 and once again with 1971-2016 (61 years). Management practices were considered to affect citrus trees and horticultural crops land uses, and their results were evaluated in terms of nitrogen loss (surface nitrogen export, which correspond to both the dissolved and sorbed nitrogen transported by overland flow and interflow, and nitrogen leaching), sediment yield (sediment exported to the lagoon) and crop yield. The model is unable to simulate crop yield within fruit trees. Thus, crop yield was evaluated only in the area covered by horticultural crops.

2.5.1 Contour farming

Contour farming (CF) consists in performing field operations (i.e., plowing, planting or sowing, cultivating and harvesting) following field contours around the slope. It prevents soil erosion, especially with storm events, and its effect was introduced into the model by modifying the P-factor map of the sediment sub-model. Factor P value in the agricultural areas with nonwoody crops (i.e., horticultural crops) was calculated according to Panagos et al. (2015) as:

$$P = P_c \, P_{sw} \, P_{vm} \qquad Eq(9)$$

where P is the support practice factor, P_c is the contouring subfactor, P_{sw} is the stone walls sedimentation subfactor (i.e., terrace sub-factor) and P_{vm} is the vegetated margins sub-factor. The slope in these areas is 3-8% and, according to Wischmeier and Smith (1978), the P_c subfactor took a value of 0.5, while the other subfactors were set at 1 because this scenario considered neither terraces nor vegetated margins (Table 3).

Scenario	P_c	P_{sw}	P_{vm}	P
Baseline	1	1	1	1
CF	0.5	1	1	0.5
CF+GFB	0.5	1	0.66	0.33
CF+HFB	0.5	1	0.09	0.045

Table 3 Final factor P and P_c, P_{sw} and P_{vm} subfactors values in the horticultural crops land use. CF: contour farming; CF+GFB: contour farming and grassy field borders; CF+HFB: contour farming and hedgerow field borders.

2.5.2 Contour farming and grassy field borders

This combination (CF+GFB) consists in carrying out contour farming and installing grassy field borders along the perimeter of fields. These grassy field borders are linear areas of herbaceous perennial species. Their installation reduces flow velocity and, consequently, soil erosion, as well as sediment and nutrient transport, because they are trapped when reaching the edge-of-the-field vegetated margin.

This effect was also introduced into the model by modifying the factor P map in the agricultural areas with nonwoody crops according to Panagos et al. (2015). The P_c and P_{sw} subfactors took the same value as in the CF scenario (Table 3). The P_{vm} subfactor took a value of 0.66 according to Panagos et al. (2015) and sediment interception was 55% for a grass border of 2 m width, which corresponded to a P_{vm} of 0.45 according to Van Vooren et al. (2017). In order to not overestimate its effectiveness, the 0.66 value with a common grass border of 2 m width was adopted (Table 3).

The area covered by grassy borders was calculated according to the borders length estimated by Rey Benayas et al. (2017). According to these authors, there are four different priority borders in an agricultural plot where grassy borders can be placed. Priority borders 1, 2 and 4 of Rey Benayas et al. (2017) are those established in CARM

(2018, 2017) proposal. Hence a total borders length of 393,549 m and 2 m width was considered.

2.5.3 Contour farming and hedgerow field borders

This second combination (CF+HFB) consists in carrying out contour farming and installing hedgerow field borders along the perimeter of fields. These hedgerow field borders are perennial woody and nonwoody structures consisting of herbaceous species, shrubs and trees that reduce flow velocity, and sediment and nutrient transport.

Likewise, the P-factor map of the sediment sub-model was modified according to Panagos et al. (2015) in the agricultural areas with nonwoody crops. The P_c and P_{sw} subfactors took the same values (Table 3) and, according to Van Vooren et al. (2017), sediment interception was estimated as 91%, and hedgerow width was not an explanatory variable. Therefore, the P_{vm} subfactor took a value of 0.09 (Table 3). As estimated by Rey Benayas et al. (2017) and proposed by CARM (2018, 2017), a total borders length of 393,549 m and 2.5 m width was considered.

2.5.4 Coastal line buffer

These scenarios consist in removing the agricultural nonwoody crops in 100 m (CB100) and 500 m (CB500) coastal line buffers. In the long-term, this abandoned land will be overgrown with herbaceous vegetation and scarce shrubs (i.e., natural grasslands). Due to crop removal, these areas remain unfertilized and, thus, nutrient transport is reduced in the most vulnerable area, which is the coast. The CB100 scenario only affected 0.08 km^2, while the CB500 scenario affected 1.53 km^2 (Figure 9) as the coast in this area is considerably urbanized. This effect was introduced into the model as a land use change.

Figure 9 Land use maps of the CB100 and CB500 scenarios.

2.5.5 Fertilizer management

Fertilizer management (FM) consists in reducing nitrogen excess by rationally controlling fertilizer doses. Fertilizer doses reduction was based on a simple soil-plant

nitrogen mass balance, which affected citrus and horticultural land uses. As the area covered by the golf course was not significant (< 2.5% of the area), the fertilizer doses in this area were not reduced. This mass balance was applied as stated in the official regulation of 2017 (CARM, 2017) and fertilizer doses were calculated as:

$$Fert = D_{max} - N_{ini} - N_{min} - N_{org} - N_{irr} \qquad Eq(10)$$

where *Fert* is the total inorganic fertilizer amount (kgN ha^{-1}), D_{max} is the maximum recommended fertilizer dose for a specific crop (kgN ha^{-1}), N_{ini} is mineral nitrogen soil content before planting (kgN ha^{-1}), N_{min} is the nitrogen that results from the organic matter mineralization process between plant and harvest dates (kgN ha^{-1}), N_{org} is the organic fertilizer (kgN ha^{-1}) and N_{irr} is the nitrogen amount in the irrigation water (kgN ha^{-1}).

In this case, N_{org} took a zero value because no organic fertilizer was used. N_{irr} was considered to be included in the term FERT because it is difficult to know the nitrogen content of irrigation water. Therefore, the fertilizer amount calculated herein included the nitrogen content of irrigation water, which farmers should deduct by means of a simple water analysis on the field scale. D_{max} was calculated according to CARM (2017), while due to the lack of data, N_{min} was calculated as the average value of the organic matter mineralization between plant and harvest dates for each crop using the baseline scenario simulation results. N_{ini} was calculated in the same way, but was corrected by a depletion coefficient, which bears in mind that nitrogen volume in soil is extremely variable, as stated in CARM (2017). It took a value of 14% in horticultural crops and 10% in citrus trees. Moreover, CARM (2017) establishes a 3-month crop exclusion period and, thus, the plant and harvest dates of melon and lettuce were adjusted by changing to shorter varieties. These final values are listed in Table 4 and the total fertilizer reduction in relation to the baseline scenario appears in Table 5.

	Land use		D_{max}	N_{ini}	N_{min}	Fert	Plant date	Harvest date
FM scenario	**Citrus trees**		250	0.9	11.8	238	-	-
	Horticultural crops	Broccoli	218	19.8	8.2	191	Jan 1	Apr 30
		Melon	118	20.1	1.1	97	Jun 1	Aug 16
		Lettuce	126	17.7	0.2	109	Oct 1	Dec 16
FM+CR scenario	**Citrus trees**		250	0.9	11.8	238	-	-
	Horticultural crops	Broccoli	218	22.8	8.2	187	Jan 1	Apr 30
		Melon	-	-	-	-	-	-
		Lettuce	126	21.1	0.2	105	Oct 1	Dec 16

Table 4 Nitrogen mass balance for each crop and scenario. Values expressed in kgN ha^{-1} $year^{-1}$. FM: fertilizer management; FM+CR: fertilizer management and two-crop rotation.

Land use	Baseline scenario	FM scenario		FM+CR scenario	
	Nitrogen fertilizer	Nitrogen fertilizer	% Reduc.	Nitrogen fertilizer	% Reduc.

Citrus trees		250	238	4.8	238	4.8
Horticultural crops	Broccoli	250	191	23.6	187	25.2
	Melon	130	97	25.4	-	100.0
	Lettuce	130	109	16.2	105	19.2

Table 5 Annual fertilizer doses for each crop and scenario. Fertilizer values expressed in kgN ha^{-1} $year^{-1}$. FM: fertilizer management; FM+CR: fertilizer management and two-crop rotation.

2.5.6 Fertilizer management and two-crop rotation

This combination (FM+CR) consists in reducing nitrogen excess by controlling fertilizer doses and changing the productive cultivation system from three-crop rotation to two-crop rotation, as established in the official regulation of 2018 (CARM, 2018). This new official regulation modifies the 2017 official regulation (CARM, 2017) insofar as only two crops can be cultivated the same year because, if fewer crops are cultivated, the fertilizer amount is expected to lower and, consequently, nitrogen surplus.

As in the FM scenario, fertilizer doses were adjusted according to CARM (2018). In addition, melon was selected to not be cultivated because the market price of this crop is more variable. D_{max} was calculated according to CARM (2018). N_{min} was calculated as an average value for each crop from the model simulation results in the current situation, but by excluding melon from the simulation. N_{ini} was calculated in the same way, but this value was corrected by the corresponding depletion coefficient (CARM, 2018). The obtained values are listed in Table 4, and the total fertilizer reduction in relation to the baseline scenario appears in Table 5.

3 Results and Discussion

3.1 Model implementation: baseline scenario

Figure 10 shows the results of the flood frequency analysis, in which a Two-Component Extreme Value (TCEV) distribution was used. The fitting for the calibration basin (Figure 8) was satisfactory (Figure 10), and the volume error (Table 6) between the simulated and calculated volume of the 25-year return period hydrograph was lower than 0.5% (absolute value).

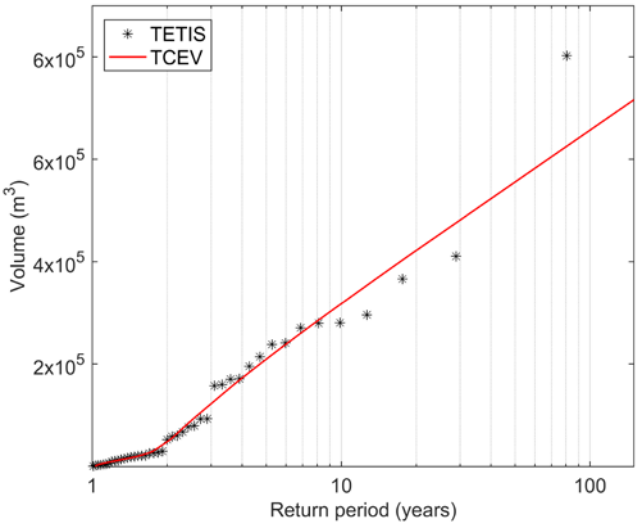

Figure 10 Flood frequency analysis results. TETIS: model simulated; TCEV: Two-Component Extreme Value adjustment.

Flood study (calculated; CAAMA, 2016a, 2016b)	457000 m^3
TETIS-N (simulated)	455016 m^3
Volume error	-0.43 %

Table 6 Calculated and simulated volume of the 25-year return period hydrograph.

On the catchment scale, the model's performance to reproduce total evapotranspiration from 2003 to 2016 was acceptable, with an R^2 value of 0.51, a KGE value of 0.45, a PBIAS of -19.31 and an RMSE value of 15.34. Moreover, it shows a good agreement between satellite-based and simulated total evapotranspiration (Figure 11).

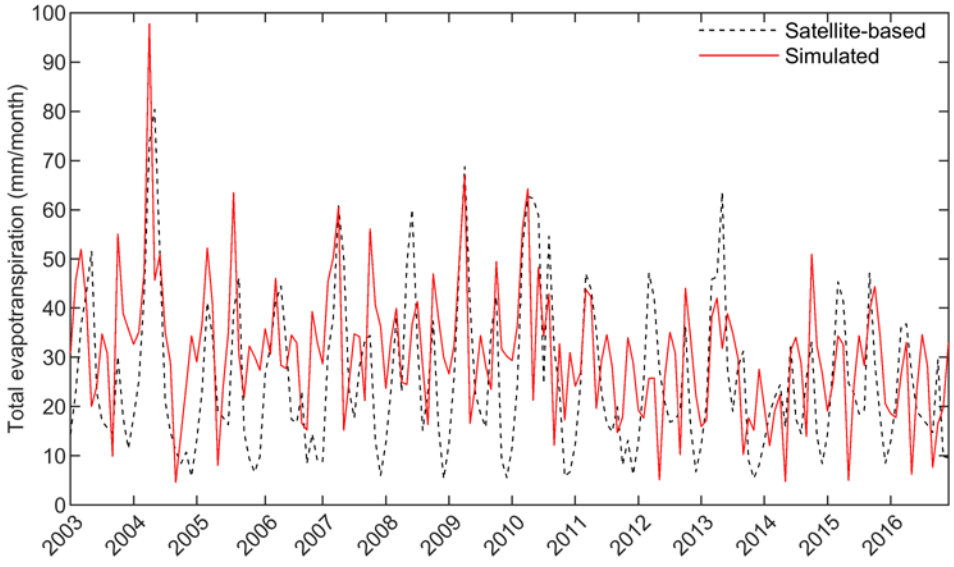

Figure 11 Satellite-based and model simulated monthly total evapotranspiration.

The mean annual results for the horticultural crop area are shown in Table 7. The difference between the evapotranspiration values under standard conditions (ET_c) and

the simulated evapotranspiration values (ET_{sim}) for lettuce was negligible. This difference was acceptable for broccoli, whereas a large difference was obtained for melon. The months from March to September (broccoli's final cultivation months and melon's complete cultivation period) correspond to dry months in this area. As shown in Table 7, irrigation+rainfall was lower than ET_c due to the limitation in the irrigation doses allocated by the Water Authority and almost no precipitation. Conversely, values close to ET_c were obtained for lettuce, which is cultivated from October to December, the rainy months. However, the transpiration requirements for each crop were approximately met because, as shown in Table 8, the simulated yield was only slightly lower than the target yield. Therefore, this difference between ET_c and ET_{sim} could be primarily attributed to lack of water to be evaporated from the uncovered part of soil in dry months because drip irrigation can induce decreased soil evaporation (Wang et al., 2020). The ET_{sim} values above irrigation+rainfall corresponded to the excess water from the previous period stored in soil.

Crop	**ET_c**	**Irrigation**	**Irrigation+Rainfall**	**ET_{real} (simulated)**
Broccoli	298.8	136.4	205.8	225.3
Melon	426.7	205.2	213.5	226.3
Lettuce	140.3	70.4	158.1	136.3

Table 7 Crop evapotranspiration, irrigation, irrigation+rainfall and real evapotranspiration (simulated) for each horticultural crop (2006-2016). Values expressed in mm $year^{-1}$.

Crop	**Target yield**	**Validation (2002-2016)**
Broccoli	8.70	7.92 (-8.6%)
Melon	1.00	0.98 (-4.9%)
Lettuce	3.30	3.13 (-5.5%)

Table 8 Target crop yield and simulated crop yield. Values in parenthesis represent mass error. Values expressed in Mg ha^{-1} $year^{-1}$.

Table 9 shows the calculated long-term annual erosion rate and the value of each USLE factor for the basin used in the calibration process (Figure 8). The volume error between the calculated and simulated mean annual erosions (Table 10) was also below 0.5% (absolute value).

A	9.29 Mg ha^{-1} $year^{-1}$
R	100 hJ cm m^{-2} h^{-1} $year^{-1}$
K	0.38 Mg m^2 h ha^{-1} hJ^{-1} cm^{-1}
LS	2.45
C	0.10
P	1

Table 9 Calculated mean annual erosion rate and values of the USLE factors.

USLE (calculated)	9.29 Mg ha^{-1} $year^{-1}$
TETIS-N (simulated)	9.27 Mg ha^{-1} $year^{-1}$
Mass error	-0.22 %

Table 10 Calculated and simulated mean annual erosion rate.

The nitrogen sub-model implementation results are shown in Table 11 and Table 10. The simulated mean annual nitrogen uptake during both the calibration and validation periods presented minor mass errors, and only the land uses mineral extraction zone and rainfed crops obtained larger differences. The mineral extraction zone presented differences smaller than 1.5 kgN ha^{-1} $year^{-1}$, which are tolerable. The elevated errors obtained for the rainfed crops were because this area remained unfertilized for modelling purposes. The difference between the estimated crop yield targets (Gallardo et al., 2011; Rincon et al., 1999; Suárez-Rey et al., 2016) and the simulated crop yields was acceptable (Table 8), with mass errors under 10% (absolute value).

Land use	Estimated uptake	Calibration (2002-2011)		Validation (2012-2016)	
Urban fabric (includes golf course)	47.4	47.2	(-0.3%)	47.7	(+0.5%)
Mineral extraction zone	3.0	4.2	(+40.0%)	4.4	(+46.7%)
Horticultural crops	460.0	455.2	(-1.0%)	462.4	(+0.5%)
Citrus trees	250.0	276.5	(+10.6%)	273.4	(+9.4%)
Rainfed crops	60.8	30.9	(-49.1%)	22.3	(-63.3%)
Forest and semi-natural areas	21.4	20.5	(-4.3%)	18.3	(-14.5%)
Sand plains	0.0	0.0	(0.0%)	0.0	(0.0%)
Salt marshes	10.0	11.5	(+15.2%)	11.3	(+13.0%)

Table 11 Estimated and simulated mean annual potential nitrogen uptake for the simplified land uses. Values in parenthesis represent mass error. Values expressed in kgN ha^{-1} $year^{-1}$.

The baseline long-term mean annual balances (61 years) are shown in Table 12. Almost all the water inputs (precipitation and irrigation) were evapotranspirated and the remaining volume was split into surface runoff and percolation. The mean annual erosion rate was quite high and, according to Albaladejo Montoro et al. (1988) it corresponds to a moderate-high erosion rate, but fell within the range of previous studies performed in southeast Spain (Boix-Fayos et al., 2005; Sougnez et al., 2011). Despite high erosion, almost all the eroded sediments were deposited, and sediment yield was much lower. The area with higher erosion rates was the mineral extraction zone, which is a very degraded area with sparse vegetation and bare soil. Nevertheless, the agricultural area still presented a mean annual erosion rate of 2.6 Mg ha^{-1}, which should be lowered because agricultural soils present high organic matter and nutrients contents (García-Ruiz et al., 2015; Merchán et al., 2018).

Water balance (mm)	
Precipitation	280.9
Irrigation	178.9
Evapotranspiration	392.6
Percolation	34.2
Surface runoff	32.9
Sediment balance (Mg ha^{-1})	

Erosion	37.2
Deposition	30.8
Sediment yield	6.3
Nitrogen balance (kgN ha^{-1})	
Fertilizer addition	206.8
Atmospheric deposition	9.1
Net mineralization	17.3
Plant nitrogen uptake	220.0
Nitrogen leaching	11.8
Surface nitrogen export	1.7

Table 12 Baseline scenario long-term mean annual balances in the soil (water, sediments and nitrogen).

The main nitrogen input was fertilizer addition and the main output was plant nitrogen uptake, which was slightly lower. This nitrogen surplus is removed from the soil due to surface runoff and percolation during high precipitation events and, although the obtained surface water runoff and percolation flows were similar (33-34 mm), the difference between surface nitrogen export (1.7 kgN ha^{-1} year^{-1}) and nitrogen leaching (11.8 kgN ha^{-1} year^{-1}) was elevated. This is a common situation in intensive agriculture (Pärn et al., 2012; Randall and Mulla, 2001) and, in this case, the higher nitrogen leaching values were obtained in agricultural areas (Figure 12). It should be highlighted that García-Pintado et al. (2007) obtained a similar value for total nitrogen export, estimated at 171 MgN year^{-1} for the whole watershed which, by considering a total area of 1200 km^2, would correspond to 1.4 kgN ha^{-1} year^{-1}.

Figure 12 Total nitrogen leaching for the baseline scenario. Values in kgN ha^{-1} year^{-1}.

By taking into account lack of data and that model implementation was used only to run model simulations to obtain a baseline scenario and projections of different ecosystem behaviours with best management scenarios (Özcan et al., 2017a), the model implementation results were considered satisfactory.

3.2 Evaluation of best management practices scenarios

An overview of the effectiveness of all the management practices scenarios is shown in Figure 13. Nitrogen loss and sediment yield were widely variable between scenarios.

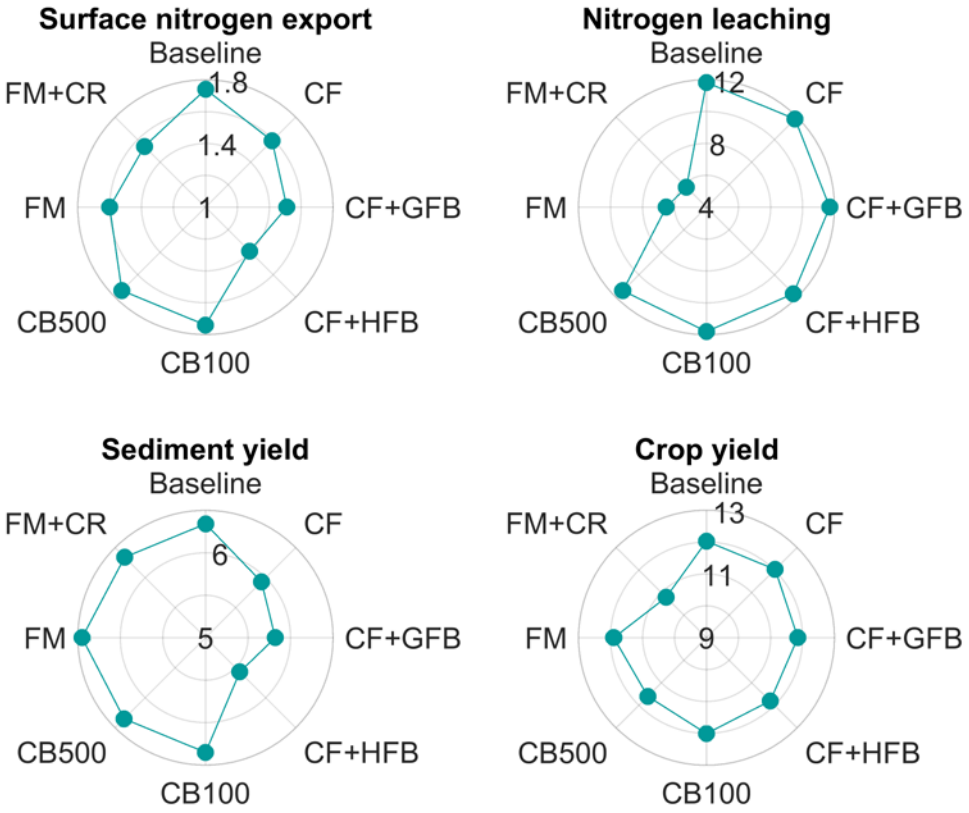

Figure 13 Surface nitrogen export (kgN ha^{-1} $year^{-1}$), nitrogen leaching (kgN ha^{-1} $year^{-1}$), sediment yield (Mg ha^{-1} $year^{-1}$) and crop yield (Mg ha^{-1} $year^{-1}$) for each management practice scenario and the baseline scenario.

In sediment yield terms, the scenarios to change the field operation management strategies (CF, CF+GFB and CF+HFB) were the most effective (Figure 13), which led to percentage reductions of 6.5%, 8.3% and 12.1% respectively, while no significant impact on crop yield was observed (Table 13). The effectiveness of these management strategies has been previously and widely analysed under different climates with similar results. López-Ballesteros et al. (2019) found that it was possible to reduce sediment yield by 6% in one of the basins in the study area by applying contour farming. This reduction could reach 7% if it was combined with hedgerow field borders of 3 m width. Arabi et al. (2008) obtained 5% percentage reductions for contour farming and 3% for vegetated field borders (5 m width). Likewise, Lam et al. (2011) considered installing of vegetative filter strips (10 m width), whose effectiveness can be compared to that of grassy field borders (Arabi et al., 2008), and they reduced sediment yield by 4.9%. Hence contour farming combined with the installation of hedgerow field borders may be the best strategy. Nonetheless, farmers may not be willing to install hedgerow field borders as it

reduces cultivation areas, and filter strips, which are installed along stream edges, are significantly more effective per unit area (Arabi et al., 2008).

The other scenarios results showed a negligible impact on sediment yield, except for the FM scenario which has a negative impact (Figure 13). As the lettuce harvest date was brought forward (Table 4) in December no crop was planted, which increased runoff and, consequently, soil erosion and sediment yield, with a value of 1.74%.

Scenario	Baseline crop yield	Percent change (%)						
		CF	CF+GFB	CF+HFB	CB100	CB500	FM	FM+CR
Broccoli	7.90	0.00	-1.46	-1.83	-0.17	-3.55	-0.97	-3.28
Melon	1.00	0.00	-1.46	-1.83	-0.17	-3.55	-3.59	-100.00
Lettuce	3.10	0.00	-1.46	-1.83	-0.17	-3.55	-0.38	-0.06
Total yield	12.00	0.00	-1.46	-1.83	-0.17	-3.55	-1.03	-10.29

Table 13 Baseline crop yield (Mg ha^{-1} $year^{-1}$) and crop yield percentage reductions for each management practice scenario.

The scenarios to change field operation management strategies (CF, CF+GFB and CF+HFB) and the scenarios which considerably reduced the total fertilizer amount (FM and FM+CR) were effective in lowering surface nitrogen export (Figure 13), although each scenario was effective in diminishing a different nitrogen form (Table 14). The CF, CF+GFB and CF+HFB scenarios were more effective in reducing organic nitrogen and sorbed $N\text{-}NH_4^+$ (Table 14) because these nitrogen forms are fixed to sediment and their mobilization is associated with soil erosion and sediment yield, while $N\text{-}NO_3^-$ is more prone to be lost by leaching than via surface runoff (Randall and Mulla, 2001). This effect was also observed by Himanshu et al. (2019), who found that contour farming and filter strips led to higher percentage reductions in organic nitrogen than $N\text{-}NO_3^-$. Conversely, the FM and FM+CR scenarios were effective in reducing $N\text{-}NO_3^-$. As fertilizer doses were adjusted to real crop requirements and distributed according to their growing curve, the $N\text{-}NO_3^-$ available to be mobilized by surface runoff considerably reduced, which consequently led to major surface $N\text{-}NO_3^-$ export reductions. However, the FM scenario slightly increased the surface organic nitrogen export because surface runoff rose. The FM+CR scenario obtained a significant crop yield reduction (Table 13). As the agricultural area affected by both coastal line buffers (CB100 and CB500) is reduced, their effect on lowering surface nitrogen export was negligible (Table 14).

Scenario	Baseline surface nitrogen export	Percent change (%)						
		CF	CF+GFB	CF+HFB	CB100	CB500	FM	FM+CR
Diss. $N\text{-}NH_4^+$	0.17	-0.06	-1.16	-1.11	0.00	-0.01	-0.13	-0.21
$N\text{-}NO_3^-$	0.85	-1.28	-2.85	-3.81	0.00	-0.05	-21.58	-23.59

OrgN	0.72	-19.58	-28.19	-44.06	+0.02	+0.20	+5.77	-0.03
Sorbed N-NH_4^+	0.01	-12.61	-18.02	-25.86	-0.01	-0.20	-3.67	-7.79
Total Nitrogen	1.74	-8.73	-13.16	-20.19	+0.01	+0.06	-8.13	-11.51

Table 14 Baseline surface nitrogen export (kgN ha^{-1} $year^{-1}$) and surface nitrogen export percentage reductions for each management practice scenario.

The CF, CF+GFB and CF+HFB scenarios obtained percentage reductions of 8.7%, 13.3% and 20.2% of the total surface nitrogen export, respectively (Table 14). Similarly, Giri et al. (2014) found that contour farming was statistically significant for reducing nitrogen yield. Haas et al. (2017) reported that filter strips of 1.5 and 3 m widths could reduce nitrogen export by 3.9% and 5.8%, respectively. Lam et al. (2011) published how the effectiveness of a 10 m width filter strip was 12.9%. All these values are similar to those herein obtained.

The FM and FM+CR scenarios, which represent total fertilizer reductions of 16.5% and 30.3%, reduced surface nitrogen export by 8.1% and 11.5% (Table 14), respectively. Lam et al. (2011) applied a 20% fertilizer reduction and found that nitrogen export could be reduced by 8.6%. Jang et al. (2017) considered 10%, 20% and 30% fertilizer reductions and lowered nitrogen export by 5.2%, 10.5% and 15.6%, respectively, Özcan et al. (2017b) proposed a 30% fertilizer reduction and obtained a 6.0% nitrogen export reduction. Cavero et al. (2012) applied fertilizer doses at optimum rates and reduced nitrogen export by 17%. So, although different effectiveness is obtained depending on specific watershed characteristics, fertilizer reductions are efficient in lowering surface nitrogen export.

Scenario	**Baseline nitrogen leaching**	**Percent change (%)**						
		CF	**CF+GFB**	**CF+HFB**	**CB100**	**CB500**	**FM**	**FM+CR**
Diss. N-NH_4^+	0.26	0.00	-2.20	-2.61	-0.04	-0.99	-1.46	-5.37
N-NO_3^-	11.55	+0.04	-1.08	-1.26	-0.12	-3.46	-45.83	-52.09
Total Nitrogen	11.82	+0.04	-1.11	-1.29	-0.12	-3.41	-44.84	-51.05

Table 15 Baseline nitrogen leaching (kgN ha^{-1} $year^{-1}$) and nitrogen leaching percentage reductions for each management practice scenario.

Finally, Table 15 shows the effectiveness of each scenario in reducing nitrogen leaching, a very important factor, because direct groundwater discharge has been recognized as the main source of nutrients (Jiménez-Martínez et al., 2016). Only the FM and FM+CR scenarios presented a noteworthy impact. The CB500 scenario showed a positive impact in reducing nitrogen leaching, but this impact was negligible compared to the FM and FM+CR scenarios. The FM scenario was able to reduce N-NO_3^- leaching

by 45.8% and total nitrogen leaching by 44.8%, while the FM+CR scenario did so by 52.1% and 51.0%, respectively. De Paz and Ramos (2004) applied a similar method (N_{min} method) and found that $N\text{-}NO_3^-$ leaching could be reduced by 66%, and barely lowered nitrogen crop uptake. Hence both scenarios FM and FM+CR showed the possibility of incrementing nitrogen use efficiency by employing residual soil nitrogen, as previously found by Dutta et al., (2017).

However, the FM+CR scenario had a significant impact on crop yield (Table 13); while the FM scenario had no significant impact. Above the strictly nitrogen crop requirement, crop yield levels off at the maximum and leaching gradually increases as more fertilizer is applied over the requirement without increasing crop yield (Giménez et al., 2016; He et al., 2012). Hence, the need to strike an equilibrium (Kropp et al., 2019) and, accordingly , reducing the fertilizer amount in scenario FM had no significant impact on crop yield, but obtained similar $N\text{-}NO_3^-$ and total nitrogen leaching reductions to the FM+CR scenario (Figure 14 and Figure 15).

The impact of both scenarios was negligible for $N\text{-}NH_4^+$ because it is easily nitrified and attracted to the negatively charged surfaces of clays and humus, which partially protect it from leaching (Porporato et al., 2003).

Figure 14 Total nitrogen leaching for the FM scenario. Values in kgN ha^{-1} $year^{-1}$.

754
755 **Figure 15** Total nitrogen leaching for the FM+CR scenario. Values in kgN ha^{-1} $year^{-1}$.

756 ## 4 Conclusions

757 In this study, the effectiveness of several management practices was evaluated in
758 terms of sediment yield, surface nitrogen export, nitrogen leaching and crop yield at the
759 Mar Menor semiarid coastal watershed.

760 The results suggest that contour farming is crucial as it achieves a major reduction
761 with no impact on crop yield, while its combination with hedgerow field borders was the
762 best option from the ecosystem point of view. Nevertheless, from the farmers point of
763 view, filter strips along the edge of streams, whose effectiveness per unit area is higher,
764 may be a better option. Regarding surface nitrogen export, the contour farming and
765 hedgerow field borders combination was very effective in reducing organic nitrogen and
766 sorbed $N\text{-}NH_4^+$ export, which are nitrogen forms highly related to soil erosion and
767 sediment yield, while the scenarios for lowering the amount of applied fertilizer were the
768 most effective in reducing the surface $N\text{-}NO_3^-$ export. Nonetheless, the differences
769 between both fertilizer management scenarios were negligible considering the marked
770 crop yield reduction due to the change in the productive cultivation system from three-
771 crop rotation to two-crop rotation, and performing fertilizer management with three-crop
772 rotation as an adequate choice. Additionally, these two scenarios significantly reduced
773 nitrogen leaching. However, due to the marked crop yield reduction, the fertilizer
774 management with three-crop rotation remains an adequate choice. The effectiveness of
775 both coastal line buffers was completely insignificant.

776 Given all these results, each management practice is effective in reducing a certain
777 diffuse pollution type and, therefore, combined scenarios are necessary to cope with all
778 agricultural pollution sources. Thus, contour farming and hedgerow field borders

779 combined with an effective fertilizer management strategy is an appropriate scenario to
780 reduce diffuse pollution.

781 ## Acknowledges

782 This work was supported by the Spanish Ministry of Science and Innovation through
783 the research projects: TETISMED (CGL2014-58127-C3-3-R) and TETISCHANGE
784 (RTI2018-093717-B-100), and by the General Directorate of Environment of the
785 Regional Government of Murcia (CARM). Authors acknowledge Faustino Martínez
786 Fernández from CARM for giving them the opportunity to develop this study and his
787 ongoing support.

788 ## References

789 Alatorre, L.C., Beguería, S., García-Ruiz, J.M., 2010. Regional scale modeling of
790 hillslope sediment delivery: A case study in the Barasona Reservoir watershed
791 (Spain) using WATEM/SEDEM. J. Hydrol. 391, 109–123.
792 https://doi.org/10.1016/j.jhydrol.2010.07.010
793 Albaladejo Montoro, J., Ortiz Silla, R., Martinez-Mena Garcia, M., 1988. Evaluation and
794 mapping of erosion risks: An example from S.E. Spain. Soil Technol. 1, 77–87.
795 https://doi.org/10.1016/S0933-3630(88)80007-2
796 Albornoz, F., Lieth, J.H., 2016. Daily macronutrient uptake patterns in relation to plant
797 age in hydroponic lettuce. J. Plant Nutr. 39, 1357–1364.
798 https://doi.org/10.1080/01904167.2015.1109110
799 Alcolea, A., Contreras, S., Hunink, J.E., García-Aróstegui, J.L., Jiménez-Martínez, J.,
800 2019. Hydrogeological modelling for the watershed management of the Mar Menor
801 coastal lagoon (Spain). Sci. Total Environ. 663, 901–914.
802 https://doi.org/10.1016/j.scitotenv.2019.01.375
803 Allen, R.G., Pereira, L.S., Raes, D., Smith, M., 1998. Crop evapotranspiration:
804 Guidelines for computing crop water requirements. Irrigation and Drainage Paper.
805 56, FAO.
806 Álvarez-Rogel, J., Jiménez-Cárceles, F.J., Nicolás, C.E., 2006. Phosphorus and nitrogen
807 content in the water of a coastal wetland in the Mar Menor lagoon (Se Spain):
808 Relationships with effluents from urban and agricultural areas. Water. Air. Soil
809 Pollut. 173, 21–38. https://doi.org/10.1007/s11270-005-9020-y
810 Álvarez, X., Valero, E., Santos, R.M.B., Varandas, S.G.P., Sanches Fernandes, L.F.,
811 Pacheco, F.A.L., 2017. Anthropogenic nutrients and eutrophication in multiple land
812 use watersheds: Best management practices and policies for the protection of water
813 resources. Land use policy 69, 1–11.
814 https://doi.org/10.1016/j.landusepol.2017.08.028
815 Arabi, M., Frankenberger, J.R., Engel, B.A., Arnold, J.G., 2008. Representation of

agricultural conservation practices with SWAT. Hydrol. Process. 22, 3042–3055. https://doi.org/10.1002/hyp.6890

Ballabio, C., Panagos, P., Monatanarella, L., 2016. Mapping topsoil physical properties at European scale using the LUCAS database. Geoderma 261, 110–123. https://doi.org/10.1016/j.geoderma.2015.07.006

Boix-Fayos, C., Martínez-Mena, M., Calvo-Cases, A., Castillo, V., Albaladejo, J., 2005. Concise review of interrill erosion studies in SE Spain (Alicante and Murcia): Erosion rates and progress of knowledge from the 1980's. L. Degrad. Dev. https://doi.org/10.1002/ldr.706

Brady, N.C., Weil, R.R., 2002. The nature and properties of soils, 13th ed. Upper Saddle River, New Jersey: Prentice-Hall.

Britto, D.T., Kronzucker, H.J., 2013. Ecological significance and complexity of N-source preference in plants. Ann. Bot. 112, 957–963. https://doi.org/10.1093/aob/mct157

Bussi, G., Francés, F., Montoya, J.J., Julien, P.Y., 2014. Distributed sediment yield modelling: Importance of initial sediment conditions. Environ. Model. Softw. 58, 58–70. https://doi.org/10.1016/j.envsoft.2014.04.010

Bussi, G., Rodríguez-Lloveras, X., Francés, F., Benito, G., Sánchez-Moya, Y., Sopeña, A., 2013. Sediment yield model implementation based on check dam infill stratigraphy in a semiarid Mediterranean catchment. Hydrol. Earth Syst. Sci. 17, 3339–3354. https://doi.org/10.5194/hess-17-3339-2013

CAAMA, 2016a. Proyecto de acciones correctoras frente al riesgo de inundación en el entorno de las urbanizaciones de Islas Menores y Mar de Cristal. T.M. Cartagena (Murcia). Consejería de Agua, Agricultura y Medio Ambiente. Región de Murcia.

CAAMA, 2016b. Proyecto de acciones correctoras frente al riesgo de inundación en el entorno de la urbanización de Los Nietos. T.M. Cartagena (Murcia). Consejería de Agua, Agricultura y Medio Ambiente. Región de Murcia.

Calatrava, J., Barberá, G.G., Castillo, V.M., 2011. Farming practices and policy measures for agricultural soil conservation in semi-arid Mediterranean areas: The case of the Guadalentín basin in southeast Spain. L. Degrad. Dev. 22, 58–69. https://doi.org/10.1002/ldr.1013

CARM, 2018. Ley 1/2018, de 7 de febrero, de medidas urgentes para garantizar la sostenibilidad ambiental en el entorno del Mar Menor. Comunidad Autónoma de la Región de Murcia.

CARM, 2017. Decreto-Ley nº. 1/2017, de 4 de abril, de medidas urgentes para garantizar la sostenibilidad ambiental en el entorno del Mar Menor. Comunidad Autónoma de la Región de Murcia.

Causapé, J., Quílez, D., Aragüés, R., 2004. Assessment of irrigation and environmental

quality at the hydrological basin level. II. Salt and nitrate loads in irrigation return flows. Agric. Water Manag. 70, 211–228. https://doi.org/10.1016/j.agwat.2004.06.006

Cavero, J., Barros, R., Sellam, F., Topcu, S., Isidoro, D., Hartani, T., Lounis, A., Ibrikci, H., Cetin, M., Williams, J.R., Aragüés, R., 2012. APEX simulation of best irrigation and N management strategies for off-site N pollution control in three Mediterranean irrigated watersheds. Agric. Water Manag. 103, 88–99. https://doi.org/10.1016/j.agwat.2011.10.021

Chiang, L.C., Chaubey, I., Maringanti, C., Huang, T., 2014. Comparing the selection and placement of best management practices in improving water quality using a multiobjective optimization and targeting method. Int. J. Environ. Res. Public Health 11, 2992–3014. https://doi.org/10.3390/ijerph110302992

Chukalla, A.D., Krol, M.S., Hoekstra, A.Y., 2018. Grey water footprint reduction in irrigated crop production: Effect of nitrogen application rate, nitrogen form, tillage practice and irrigation strategy. Hydrol. Earth Syst. Sci. 22, 3245–3259. https://doi.org/10.5194/hess-22-3245-2018

Clapp, R.B., Hornberger, G.M., 1978. Empirical equations for some soil hydraulic properties. Water Resour. Res. 14, 601–604. https://doi.org/10.1029/WR014i004p00601

Collins, A.L., Naden, P.S., Sear, D.A., Jones, J.I., Foster, I.D.L., Morrow, K., 2011. Sediment targets for informing river catchment management: international experience and prospects. Hydrol. Process. 25, 2112–2129. https://doi.org/10.1002/hyp.7965

D'Odorico, P., Laio, F., Porporato, A., Rodriguez-Iturbe, I., 2003. Hydrologic controls on soil carbon and nitrogen cycles. II. A case study. Adv. Water Resour. 26, 59–70. https://doi.org/10.1016/S0309-1708(02)00095-7

De Pascalis, F., Pérez-Ruzafa, A., Gilabert, J., Marcos, C., Umgiesser, G., 2012. Climate change response of the Mar Menor coastal lagoon (Spain) using a hydrodynamic finite element model. Estuar. Coast. Shelf Sci. 114, 118–129. https://doi.org/10.1016/j.ecss.2011.12.002

De Paz, J.M., Ramos, C., 2004. Simulation of nitrate leaching for different nitrogen fertilization rates in a region of Valencia (Spain) using a GIS-GLEAMS system. Agric. Ecosyst. Environ. 103, 59–73. https://doi.org/10.1016/j.agee.2003.10.006

De Paz, J.M., Ramos, C., 2002. Linkage of a geographical information system with the gleams model to assess nitrate leaching in agricultural areas, in: Environmental Pollution. Elsevier, pp. 249–258. https://doi.org/10.1016/S0269-7491(01)00317-7

Dechmi, F., Skhiri, A., 2013. Evaluation of best management practices under intensive

irrigation using SWAT model. Agric. Water Manag. 123, 55–64. https://doi.org/10.1016/j.agwat.2013.03.016

Dutta, B., Grant, B.B., Campbell, C.A., Lemke, R.L., Desjardins, R.L., Smith, W.N., 2017. A multi model evaluation of long-term effects of crop management and cropping systems on nitrogen dynamics in the Canadian semi-arid prairie. Agric. Syst. 151, 136–147. https://doi.org/10.1016/j.agsy.2016.12.003

Engelund, F., Hansen, E., 1972. A Monograph on Sediment Transport in Alluvial Streams, Technical University of Denmark, Hydraulic Laboratory. TEKNISKFORLAG Skelbrekgade 4 Copenhagen V, Denmark.

Francés, F., Vélez, J.I., Vélez, J.J., 2007. Split-parameter structure for the automatic calibration of distributed hydrological models. J. Hydrol. 332, 226–240. https://doi.org/10.1016/J.JHYDROL.2006.06.032

Gallardo, M., Giménez, C., Martínez-Gaitán, C., Stöckle, C.O., Thompson, R.B., Granados, M.R., 2011. Evaluation of the VegSyst model with muskmelon to simulate crop growth, nitrogen uptake and evapotranspiration. Agric. Water Manag. 101, 107–117. https://doi.org/10.1016/j.agwat.2011.09.008

Garcia-Ayllon, S., 2018. The Integrated Territorial Investment (ITI) of the Mar Menor as a model for the future in the comprehensive management of enclosed coastal seas. Ocean Coast. Manag. 166, 82–97. https://doi.org/10.1016/j.ocecoaman.2018.05.004

García-Ayllón, S., Miralles, J.L., 2014. The environmental impacts of land transformation in the coastal perimeter of the mar menor lagoon (SPAIN). Int. J. Des. Nat. Ecodynamics 9, 109–128. https://doi.org/10.2495/DNE-V9-N2-109-128

García-Gómez, H., Garrido, J.L., Vivanco, M.G., Lassaletta, L., Rábago, I., Àvila, A., Tsyro, S., Sánchez, G., González Ortiz, A., González-Fernández, I., Alonso, R., 2014. Nitrogen deposition in Spain: Modeled patterns and threatened habitats within the Natura 2000 network. Sci. Total Environ. 485–486, 450–460. https://doi.org/10.1016/J.SCITOTENV.2014.03.112

García-Pintado, J., Martínez-Mena, M., Barberá, G.G., Albaladejo, J., Castillo, V.M., 2007. Anthropogenic nutrient sources and loads from a Mediterranean catchment into a coastal lagoon: Mar Menor, Spain. Sci. Total Environ. 373, 220–239. https://doi.org/10.1016/j.scitotenv.2006.10.046

García-Ruiz, J.M., Beguería, S., Nadal-Romero, E., González-Hidalgo, J.C., Lana-Renault, N., Sanjuán, Y., 2015. A meta-analysis of soil erosion rates across the world. Geomorphology 239, 160–173. https://doi.org/10.1016/j.geomorph.2015.03.008

Giménez, C., Stöckle, C.O., Suárez-Rey, E.M., Gallardo, M., 2016. Crop yields and N

927 losses tradeoffs in a garlic-wheat rotation in southern Spain. Eur. J. Agron. 73, 160–
928 169. https://doi.org/10.1016/j.eja.2015.11.016
929 Giri, S., Nejadhashemi, A.P., 2014. Application of analytical hierarchy process for
930 effective selection of agricultural best management practices. J. Environ. Manage.
931 132, 165–177. https://doi.org/10.1016/j.jenvman.2013.10.021
932 Giri, S., Nejadhashemi, A.P., Woznicki, S., Zhang, Z., 2014. Analysis of best
933 management practice effectiveness and spatiotemporal variability based on
934 different targeting strategies. Hydrol. Process. 28, 431–445.
935 https://doi.org/10.1002/hyp.9577
936 Haas, M.B., Guse, B., Fohrer, N., 2017. Assessing the impacts of Best Management
937 Practices on nitrate pollution in an agricultural dominated lowland catchment
938 considering environmental protection versus economic development. J. Environ.
939 Manage. 196, 347–364. https://doi.org/10.1016/j.jenvman.2017.02.060
940 Hargreaves, G.H., Samani, Z.A., 1985. Reference Crop Evapotranspiration from
941 Temperature. Appl. Eng. Agric. 1, 96–99. https://doi.org/10.13031/2013.26773
942 Harrison, S., McAree, C., Mulville, W., Sullivan, T., 2019. The problem of agricultural
943 'diffuse' pollution: Getting to the point. Sci. Total Environ. 677, 700–717.
944 https://doi.org/10.1016/J.SCITOTENV.2019.04.169
945 Hashemi, F., Olesen, J.E., Dalgaard, T., Børgesen, C.D., 2016. Review of scenario
946 analyses to reduce agricultural nitrogen and phosphorus loading to the aquatic
947 environment. Sci. Total Environ. 573, 608–626.
948 https://doi.org/10.1016/j.scitotenv.2016.08.141
949 He, J., Dukes, M.D., Hochmuth, G.J., Jones, J.W., Graham, W.D., 2012. Identifying
950 irrigation and nitrogen best management practices for sweet corn production on
951 sandy soils using CERES-Maize model. Agric. Water Manag. 109, 61–70.
952 https://doi.org/10.1016/j.agwat.2012.02.007
953 Herrera, S., Fernández, J., Gutiérrez, J.M., 2016. Update of the Spain02 gridded
954 observational dataset for EURO-CORDEX evaluation: Assessing the effect of the
955 interpolation methodology. Int. J. Climatol. 36, 900–908.
956 https://doi.org/10.1002/joc.4391
957 Hiederer, R., 2013. Mapping Soil Properties for Europe - Spatial Representation of Soil
958 Database Attributes, JRC Technical Reports. Luxembourg: Publications Office of
959 the European Union. https://doi.org/10.2788/94128
960 Himanshu, S.K., Pandey, A., Yadav, B., Gupta, A., 2019. Evaluation of best management
961 practices for sediment and nutrient loss control using SWAT model. Soil Tillage Res.
962 192, 42–58. https://doi.org/10.1016/j.still.2019.04.016
963 Ingram, J., 2008. Agronomist-farmer knowledge encounters: An analysis of knowledge

964 exchange in the context of best management practices in England. Agric. Human
965 Values 25, 405–418. https://doi.org/10.1007/s10460-008-9134-0
966 Jang, S.S., Ahn, S.R., Kim, S.J., 2017. Evaluation of executable best management
967 practices in Haean highland agricultural catchment of South Korea using SWAT.
968 Agric. Water Manag. 180, 224–234. https://doi.org/10.1016/j.agwat.2016.06.008
969 Jiménez-Martínez, J., García-Aróstegui, J.L., Hunink, J.E., Contreras, S., Baudron, P.,
970 Candela, L., 2016. The role of groundwater in highly human-modified
971 hydrosystems: a review of impacts and mitigation options in the Campo de
972 Cartagena-Mar Menor coastal plain (SE Spain). Environ. Rev. 24, 377–392.
973 https://doi.org/10.1139/er-2015-0089
974 Julien, P.Y., 2010. Erosion and sedimentation, 2nd ed. Cambridge University Press.
975 Jung, Y.W., Oh, D.S., Kim, M., Park, J.W., 2010. Calibration of LEACHN model using
976 LH-OAT sensitivity analysis. Nutr. Cycl. Agroecosystems 87, 261–275.
977 https://doi.org/10.1007/s10705-009-9337-9
978 Kilinc, M., Richardson, E. V, 1973. Mechanics of Soil Erosion from Overland Flow
979 Generated by Simulated Rainfall. Colorado State University. Hydrology Papers.
980 Kimmins, J.P., 2004. Forest ecology: a foundation for sustainable forest management
981 and environmental ethics in forestry, 3rd ed. Upper Saddle River, New Jersey:
982 Prentice-Hall.
983 Kropp, I., Nejadhashemi, A.P., Deb, K., Abouali, M., Roy, P.C., Adhikari, U.,
984 Hoogenboom, G., 2019. A multi-objective approach to water and nutrient efficiency
985 for sustainable agricultural intensification. Agric. Syst. 173, 289–302.
986 https://doi.org/10.1016/j.agsy.2019.03.014
987 La Nauze, A., Mezzetti, C., 2019. Dynamic incentive regulation of diffuse pollution. J.
988 Environ. Econ. Manage. 93, 101–124. https://doi.org/10.1016/j.jeem.2018.11.009
989 Lam, Q.D., Schmalz, B., Fohrer, N., 2011. The impact of agricultural Best Management
990 Practices on water quality in a North German lowland catchment. Environ. Monit.
991 Assess. 183, 351–379. https://doi.org/10.1007/s10661-011-1926-9
992 Le Moal, M., Gascuel-Odoux, C., Ménesguen, A., Souchon, Y., Étrillard, C., Levain, A.,
993 Moatar, F., Pannard, A., Souchu, P., Lefebvre, A., Pinay, G., 2019. Eutrophication:
994 A new wine in an old bottle? Sci. Total Environ.
995 https://doi.org/10.1016/j.scitotenv.2018.09.139
996 León, V.M., Moreno-González, R., García, V., Campillo, J.A., 2017. Impact of flash flood
997 events on the distribution of organic pollutants in surface sediments from a
998 Mediterranean coastal lagoon (Mar Menor, SE Spain). Environ. Sci. Pollut. Res. 24,
999 4284–4300. https://doi.org/10.1007/s11356-015-4628-y
1000 Liu, R., Zhang, P., Wang, X., Chen, Y., Shen, Z., 2013. Assessment of effects of best

1001 management practices on agricultural non-point source pollution in Xiangxi River
1002 watershed. Agric. Water Manag. 117, 9–18.
1003 https://doi.org/10.1016/j.agwat.2012.10.018
1004 López-Ballesteros, A., Senent-Aparicio, J., Srinivasan, R., Pérez-Sánchez, J., 2019.
1005 Assessing the impact of best management practices in a highly anthropogenic and
1006 ungauged watershed using the SWAT model: A case study in the El beal watershed
1007 (Southeast Spain). Agronomy 9, 576. https://doi.org/10.3390/agronomy9100576
1008 Martens, B., Miralles, D.G., Lievens, H., Van Der Schalie, R., De Jeu, R.A.M.,
1009 Fernández-Prieto, D., Beck, H.E., Dorigo, W.A., Verhoest, N.E.C., 2017. GLEAM
1010 v3: Satellite-based land evaporation and root-zone soil moisture. Geosci. Model
1011 Dev. 10, 1903–1925. https://doi.org/10.5194/gmd-10-1903-2017
1012 Merchán, D., Casalí, J., Del Valle de Lersundi, J., Campo-Bescós, M.A., Giménez, R.,
1013 Preciado, B., Lafarga, A., 2018. Runoff, nutrients, sediment and salt yields in an
1014 irrigated watershed in southern Navarre (Spain). Agric. Water Manag. 195, 120–
1015 132. https://doi.org/10.1016/j.agwat.2017.10.004
1016 Mintegui, J.Á., de Simón, E., García-Rodríguez, J.L., Robredo, J.C., 1993. La
1017 restauración hidrológico-forestal en las ceuncas hidrográficas de la vertiente
1018 mediterránea. Junta de Andalucía. Consejería de Agricultura y Pesca.
1019 Miralles, D.G., Holmes, T.R.H., De Jeu, R.A.M., Gash, J.H., Meesters, A.G.C.A.,
1020 Dolman, A.J., 2011. Global land-surface evaporation estimated from satellite-based
1021 observations. Hydrol. Earth Syst. Sci. 15, 453–469. https://doi.org/10.5194/hess-
1022 15-453-2011
1023 Mtibaa, S., Hotta, N., Irie, M., 2018. Analysis of the efficacy and cost-effectiveness of
1024 best management practices for controlling sediment yield: A case study of the
1025 Joumine watershed, Tunisia. Sci. Total Environ. 616–617, 1–16.
1026 https://doi.org/10.1016/j.scitotenv.2017.10.290
1027 Özcan, Z., Başkan, O., Düzgün, H.Ş., Kentel, E., Alp, E., 2017a. A pollution fate and
1028 transport model application in a semi-arid region: Is some number better than no
1029 number? Sci. Total Environ. 595, 425–440.
1030 https://doi.org/10.1016/j.scitotenv.2017.03.240
1031 Özcan, Z., Kentel, E., Alp, E., 2017b. Evaluation of the best management practices in a
1032 semi-arid region with high agricultural activity. Agric. Water Manag. 194, 160–171.
1033 https://doi.org/10.1016/j.agwat.2017.09.007
1034 Panagos, P., Borrelli, P., Meusburger, K., van der Zanden, E.H., Poesen, J., Alewell, C.,
1035 2015. Modelling the effect of support practices (P-factor) on the reduction of soil
1036 erosion by water at European scale. Environ. Sci. Policy 51, 23–34.
1037 https://doi.org/10.1016/j.envsci.2015.03.012

1038 Panagos, P., Meusburger, K., Ballabio, C., Borrelli, P., Alewell, C., 2014. Soil erodibility
1039 in Europe: A high-resolution dataset based on LUCAS. Sci. Total Environ. 479–480,
1040 189–200. https://doi.org/10.1016/j.scitotenv.2014.02.010
1041 Pardo, G., del Prado, A., Martínez-Mena, M., Bustamante, M.A., Martín, J.A.A.R., Álvaro-
1042 Fuentes, J., Moral, R., 2017. Orchard and horticulture systems in Spanish
1043 Mediterranean coastal areas: Is there a real possibility to contribute to C
1044 sequestration? Agric. Ecosyst. Environ. 238, 153–167.
1045 https://doi.org/10.1016/j.agee.2016.09.034
1046 Pärn, J., Pinay, G., Mander, Ü., 2012. Indicators of nutrients transport from agricultural
1047 catchments under temperate climate: A review. Ecol. Indic. 22, 4–15.
1048 https://doi.org/10.1016/j.ecolind.2011.10.002
1049 Pearce, N.J.T., Yates, A.G., 2017. Intra-annual variation of the association between
1050 agricultural best management practices and stream nutrient concentrations. Sci.
1051 Total Environ. 586, 1124–1134. https://doi.org/10.1016/j.scitotenv.2017.02.102
1052 Perni, A., Martínez-Paz, J.M., 2013. A participatory approach for selecting cost-effective
1053 measures in the WFD context: The Mar Menor (SE Spain). Sci. Total Environ. 458–
1054 460, 303–311. https://doi.org/10.1016/j.scitotenv.2013.04.029
1055 Poch-Massegú, R., Jiménez-Martínez, J., Wallis, K.J., Ramírez de Cartagena, F.,
1056 Candela, L., 2014. Irrigation return flow and nitrate leaching under different crops
1057 and irrigation methods in Western Mediterranean weather conditions. Agric. Water
1058 Manag. 134, 1–13. https://doi.org/10.1016/j.agwat.2013.11.017
1059 Porporato, A., D'Odorico, P., Laio, F., Rodriguez-Iturbe, I., 2003. Hydrologic controls on
1060 soil carbon and nitrogen cycles. I. Modeling scheme. Adv. Water Resour. 26, 45–
1061 58. https://doi.org/10.1016/S0309-1708(02)00094-5
1062 Pradhan, P., Fischer, G., Van Velthuizen, H., Reusser, D.E., Kropp, J.P., 2015. Closing
1063 yield gaps: How sustainable can we be? PLoS One 10, 18.
1064 https://doi.org/10.1371/journal.pone.0129487
1065 Qiu, J., Shen, Z., Huang, M., Zhang, X., 2018. Exploring effective best management
1066 practices in the Miyun reservoir watershed, China. Ecol. Eng. 123, 30–42.
1067 https://doi.org/10.1016/j.ecoleng.2018.08.020
1068 Quemada, M., Baranski, M., Nobel-de Lange, M.N.J., Vallejo, A., Cooper, J.M., 2013.
1069 Meta-analysis of strategies to control nitrate leaching in irrigated agricultural
1070 systems and their effects on crop yield. Agric. Ecosyst. Environ. 174, 1–10.
1071 https://doi.org/10.1016/j.agee.2013.04.018
1072 Rahn, C.R., Zhang, K., Lillywhite, R., Ramos, C., Doltra, J., de Paz, J.M., Riley, H., Fink,
1073 M., Nendel, C., Thorup-Kristensen, K., Pedersen, A., Piro, F., Venezia, A., Firth, C.,
1074 Schmutz, U., Rayns, F., Strohmeyer, K., 2010. Eu-Rotate_N - a decision support

1075 system - to predict environmental and economic consequences of the management
1076 of nitrogen fertiliser in crop rotations. Eur. J. Hortic. Sci. 75, 20–32.
1077 Ramos, C., Pomares, F., 2010. Abonado de los cultivos hortícolas, in: Guía Práctica de
1078 La Fertilización Racional de Los Cultivos En España. Ministerio de Medio Ambiente
1079 y Medio Rural y Marino, p. 260.
1080 Randall, G.W., Mulla, D.J., 2001. Nitrate Nitrogen in Surface Waters as Influenced by
1081 Climatic Conditions and Agricultural Practices. J. Environ. Qual. 30, 337–344.
1082 https://doi.org/10.2134/jeq2001.302337x
1083 Rankinen, K., Karvonen, T., Butterfield, D., 2006. An application of the GLUE
1084 methodology for estimating the parameters of the INCA-N model. Sci. Total Environ.
1085 365, 123–139. https://doi.org/10.1016/J.SCITOTENV.2006.02.034
1086 Rao, N.S., Easton, Z.M., Schneiderman, E.M., Zion, M.S., Lee, D.R., Steenhuis, T.S.,
1087 2009. Modeling watershed-scale effectiveness of agricultural best management
1088 practices to reduce phosphorus loading. J. Environ. Manage. 90, 1385–1395.
1089 https://doi.org/10.1016/j.jenvman.2008.08.011
1090 Rey Benayas, J.M., Viñegla Prades, F., Mesa Fraile, A. V., 2017. Diseño de una red de
1091 setos e islotes forestales para la restauración agroecológica de la Cuenca Sur del
1092 Mar Menor (Murcia). Fundación Internacional para la Restauración de
1093 Ecosistemas, Madrid. Consejería de Agua, Agricultura y Medio Ambiente, Región
1094 de Murcia.
1095 Rey, J., Martínez, J., Barberá, G.G., García-Aróstegui, J.L., García-Pintado, J., Martínez-
1096 Vicente, D., 2013. Geophysical characterization of the complex dynamics of
1097 groundwater and seawater exchange in a highly stressed aquifer system linked to
1098 a coastal lagoon (SE Spain). Environ. Earth Sci. 70, 2271–2282.
1099 https://doi.org/10.1007/s12665-013-2472-2
1100 Rincon, L., Saez, J., Perez, J., Pellicer, C., Gomez, M., 1999. Crecimiento y Absorción
1101 de Nutrientes del Brócoli. Invest. Agr. Prod. Prot. Veg. 14, 225–236.
1102 Saxton, K.E., Rawls, W.J., 2006. Soil Water Characteristic Estimates by Texture and
1103 Organic Matter for Hydrologic Solutions. Soil Sci. Soc. Am. J. 70, 1569–1578.
1104 https://doi.org/10.2136/sssaj2005.0117
1105 Sharpley, A.N., Daniel, T., Gibson, G., Bundy, L., Cabrera, M., Sims, T., Stevens, R.,
1106 Lemunyon, J., Kleinman, P., Parry, R., 2006. Best Management Practices To
1107 Minimize Agricultural Phosphorus Impacts on Water Quality.
1108 Sith, R., Watanabe, A., Nakamura, T., Yamamoto, T., Nadaoka, K., 2019. Assessment
1109 of water quality and evaluation of best management practices in a small agricultural
1110 watershed adjacent to Coral Reef area in Japan. Agric. Water Manag. 213, 659–
1111 673. https://doi.org/10.1016/j.agwat.2018.11.014

1112 Sougnez, N., van Wesemael, B., Vanacker, V., 2011. Low erosion rates measured for
1113 steep, sparsely vegetated catchments in southeast Spain. Catena.
1114 https://doi.org/10.1016/j.catena.2010.08.010
1115 Strauch, M., Lima, J.E.F.W., Volk, M., Lorz, C., Makeschin, F., 2013. The impact of Best
1116 Management Practices on simulated streamflow and sediment load in a Central
1117 Brazilian catchment. J. Environ. Manage. 127, S24–S36.
1118 https://doi.org/10.1016/j.jenvman.2013.01.014
1119 Suárez-Rey, E.M., Romero-Gámez, M., Giménez, C., Thompson, R.B., Gallardo, M.,
1120 2016. Use of EU-Rotate_N and CropSyst models to predict yield, growth and water
1121 and N dynamics of fertigated leafy vegetables in a Mediterranean climate and to
1122 determine N fertilizer requirements. Agric. Syst. 149, 150–164.
1123 https://doi.org/10.1016/j.agsy.2016.09.007
1124 Tilman, D., Balzer, C., Hill, J., Befort, B.L., 2011. Global food demand and the
1125 sustainable intensification of agriculture. Proc. Natl. Acad. Sci. U. S. A. 108, 20260–
1126 20264. https://doi.org/10.1073/pnas.1116437108
1127 Tilman, D., Cassman, K.G., Matson, P.A., Naylor, R., Polasky, S., 2002. Agricultural
1128 sustainability and intensive production practices. Nature 418, 671–677.
1129 https://doi.org/10.1038/nature01014
1130 Tsakovski, S., Kudłak, B., Simeonov, V., Wolska, L., Garcia, G., Dassenakis, M.,
1131 Namieśnik, J., 2009. N-way modelling of sediment monitoring data from Mar Menor
1132 lagoon, Spain. Talanta 80, 935–941. https://doi.org/10.1016/j.talanta.2009.08.015
1133 Ullrich, A., Volk, M., 2009. Application of the Soil and Water Assessment Tool (SWAT)
1134 to predict the impact of alternative management practices on water quality and
1135 quantity. Agric. Water Manag. 96, 1207–1217.
1136 https://doi.org/10.1016/j.agwat.2009.03.010
1137 Van Vooren, L., Reubens, B., Broekx, S., De Frenne, P., Nelissen, V., Pardon, P.,
1138 Verheyen, K., 2017. Ecosystem service delivery of agri-environment measures: A
1139 synthesis for hedgerows and grass strips on arable land. Agric. Ecosyst. Environ.
1140 244, 32–51. https://doi.org/10.1016/j.agee.2017.04.015
1141 Velasco, J., Lloret, J., Millan, A., Marin, A., Barahona, J., Abellan, P., Sanchez-
1142 Fernandez, D., 2006. Nutrient and particulate inputs into the Mar Menor lagoon (Se
1143 Spain) from an intensive agricultural watershed. Water. Air. Soil Pollut. 176, 37–56.
1144 https://doi.org/10.1007/s11270-006-2859-8
1145 Wade, A.J., Durand, P., Beaujouan, V., Wessel, W.W., Raat, K.J., Whitehead, P.G.,
1146 Butterfield, D., Rankinen, K., Lepisto, A., 2002. A nitrogen model for European
1147 catchments: INCA, new model structure and equations. Hydrol. Earth Syst. Sci. 6,
1148 559–582. https://doi.org/10.5194/hess-6-559-2002

Wagena, M.B., Easton, Z.M., 2018. Agricultural conservation practices can help mitigate the impact of climate change. Sci. Total Environ. 635, 132–143. https://doi.org/10.1016/j.scitotenv.2018.04.110

Wang, W., Xie, Y., Bi, M., Wang, X., Lu, Y., Fan, Z., 2018. Effects of best management practices on nitrogen load reduction in tea fields with different slope gradients using the SWAT model. Appl. Geogr. 90, 200–213. https://doi.org/10.1016/j.apgeog.2017.08.020

Wang, Y., Li, S., Qin, S., Guo, H., Yang, D., Lam, H.M., 2020. How can drip irrigation save water and reduce evapotranspiration compared to border irrigation in arid regions in northwest China. Agric. Water Manag. 239. https://doi.org/10.1016/j.agwat.2020.106256

Weil, R.R., Brady, N.C., 2017. The nature and properties of soils, 15th ed. Harlow, England : Pearson Education.

Wischmeier, W.H., Smith, D.D., 1978. Predicting rainfall erosion losses - a guide to conservation planning. United States Department of Agriculture (USDA). Washington, DC, USA.

Zhang, Y., Collins, A.L., Murdoch, N., Lee, D., Naden, P.S., 2014. Cross sector contributions to river pollution in England and Wales: Updating waterbody scale information to support policy delivery for the Water Framework Directive. Environ. Sci. Policy 42, 16–32. https://doi.org/10.1016/j.envsci.2014.04.010

Zhang, Y., Zhou, Y., Shao, Q., Liu, H., Lei, Q., Zhai, X., Wang, X., 2016. Diffuse nutrient losses and the impact factors determining their regional differences in four catchments from North to South China. J. Hydrol. 543, 577–594. https://doi.org/10.1016/j.jhydrol.2016.10.031